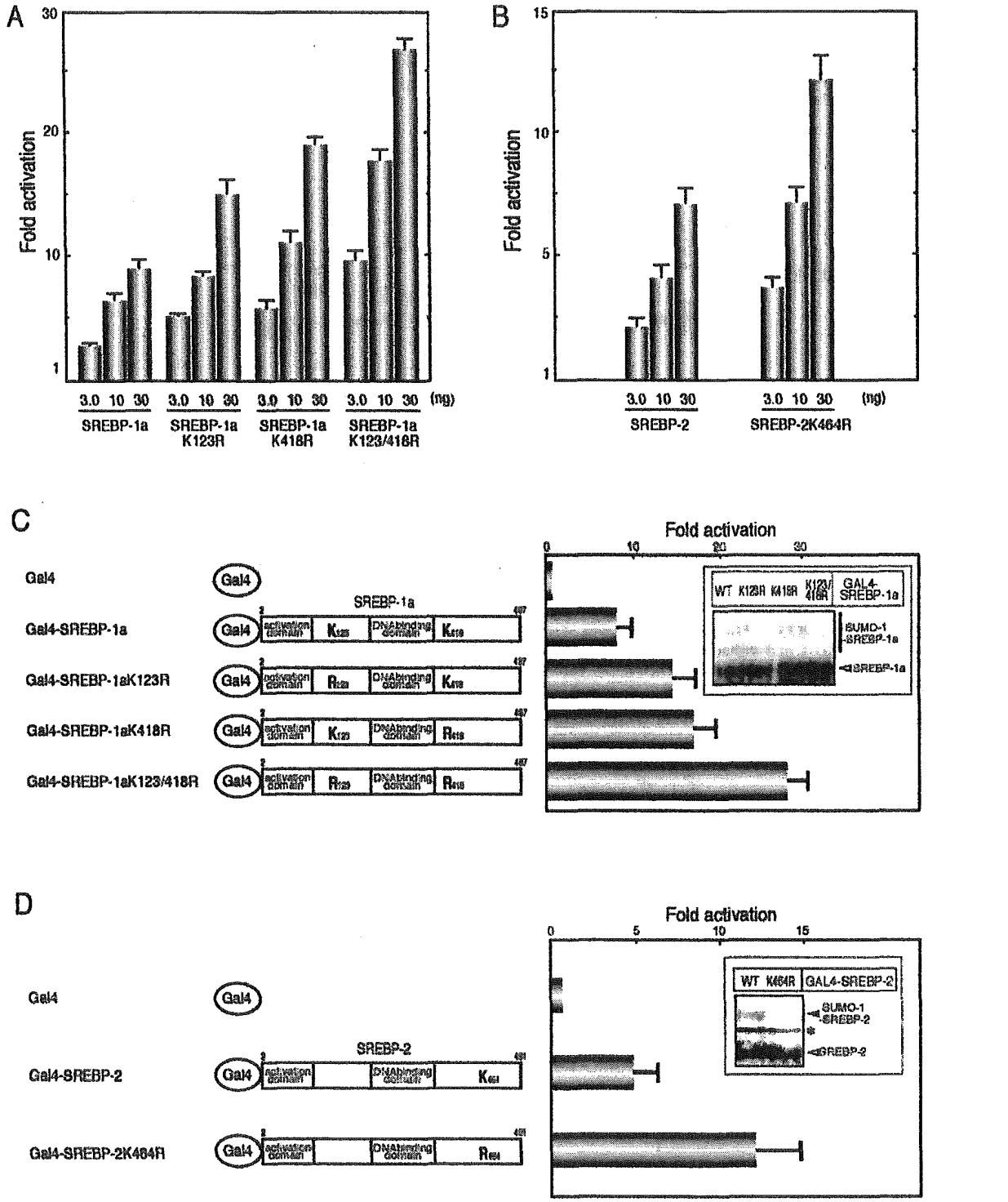

FIG. 5. **Sumoylation of SREBPs reduces their transactivation activities.** HEK293 cells were cotransfected with increasing amounts of expression plasmids encoding either wild-type or mutant versions of SREBP-1a (*A*) or SREBP-2 (*B*) or 0.03 μg of expression plasmids encoding pHA-SUMO-1 and either wild-type or mutant versions of pG4-FLSBP-1a (*C*) or pG4-HisSBP-2 (*D*) along with 0.2 μg of the reporter plasmids either pLDLR (*A* and *B*) or pG5Luc (*C* and *D*) and 0.01 μg of pRL-CMV per 35-mm dish. After 48 h of culture, luciferase assays were performed as described under "Experimental Procedures." Promoter activities in the absence of SREBP expression plasmids are set as 1. Data are mean ± S.E. values of three independent experiments performed in triplicate. Expression levels of sumoylated SREBPs were evaluated by immunoprecipitation and immunoblotting with anti-SREBP-1/2 antibodies in the cell extracts and shown *inside* the *plot area*. An *asterisk* marks the nonspecific bands observed in all lanes.

shows that Gal4-SREBP-2K464R significantly enhanced transcription of the reporter gene to an extent elicited by double mutation in SREBP-1a. These results indicate that SUMO-1 modification of SREBPs directly reduces their own transcriptional activities. On the other hand, we cannot rule out the possibility that sumoylation of SREBPs might influence their interaction with co-regulatory factors or their DNA affinity.

Effect of Sumoylation of SREBPs on Their Stability—We previously reported that nuclear SREBPs are rapidly degraded via the ubiquitin/26 S proteasome pathway (8). Since both sumoylation and ubiquitylation require a lysine residue of target proteins, we examined whether sumoylation competes with ubiquitylation, thereby affecting the ubiquitin-dependent degradation of nuclear SREBPs. Pulse-chase experiments using COS-1 cells transfected with expression plasmids encoding either FLAG-tagged wild-type or K464R SREBP-2 were performed. Fig. 6*A* shows that the calculated half-life of wild-type and K464R SREBP-2 was ~2 h and that there were no obvious differences in their stabilities. Similar results were obtained when cells were transfected with expression plasmids encoding either wild-type or mutant versions of FLAG-SREBP-1a (data not shown). Taken together, these results indicate that sumoylation of SREBPs does not influence their degradation through the ubiquitin/26 S proteasome pathway.

To directly determine whether wild-type and mutant versions of SREBPs are similarly modified by ubiquitin, we devised an *in vitro* ubiquitylation assay for SREBPs. In this system, the GST-SREBPs expressed in COS-1 cells were conjugated with glutathione-Sepharose resins and then incubated with recombinant Ub-activating enzyme (E1) and Ub-conjugating enzyme (E2) in the presence of GST-Ub and ATP. We confirmed that Ubc4, but not UbcH7, collaborates as E2 for the *in vitro* ubiquitylation assay of SREBPs (data not shown). As shown in the *top panels* of Fig. 6*B*, in the presence of Ubc4, the amounts of parental forms of SREBPs were decreased (*arrowheads*), and high molecular mass smear bands (*closed bars*) were observed by immunoblotting with anti-SREBP antibodies. To confirm that these multiple smear bands are indeed ubiquitin-modified forms of SREBPs, we performed immunoblotting with anti-multiubiquitin antibodies. High molecular mass smear bands were also detected with anti-multiubiquitin antibodies (*lower panels*). Weak ubiquitylated smear bands were observed when UbcH7 was used as E2, which probably reflected endogenously ubiquitylated SREBPs. These results allow us to conclude that wild-type and mutant versions of SREBPs are similarly modified by ubiquitin and that sumoylation does not compete with ubiquitylation in the SREBPs.

Sumoylation of SREBPs under Sterol-loaded or -depleted Conditions—Our next question was whether intracellular sterol levels alter the rate of sumoylation of SREBPs. It is possible that high sterol levels could accelerate sumoylation of nuclear SREBPs, thus suppressing the transcription of SREBP-responsive genes. To investigate this issue, we used M19 cells, which lacks site 2 protease (43), resulting in the absence of endogenous nuclear SREBPs. In these cells, one can determine sumoylation of exogenously expressed SREBPs under either sterol-depleted or sterol-loaded conditions in the absence of endogenous SREBPs. The cells were transfected with expression plasmids encoding His-SUMO-1 and GST-SREBPs and cultured under either sterol-depleted or sterol-loaded conditions. GST-SREBPs bound to glutathione-Sepharose resins were subjected to immunoblotting analysis with anti-SUMO-1 (Fig. 7, *top*) and anti-SREBP-1/2 (*bottom*) antibodies. The amounts of sumoylated and unmodified SREBPs under either sterol-loaded (*lanes 1* and *3*) or sterol-depleted (*lanes 2* and *4*) conditions were similar. These results demonstrate that sterols do not alter the sumoylation rate of SREBPs.

The SUMO-conjugating Enzyme, Ubc9, Interacts with SREBPs—To investigate the direct interaction of SREBP with endogenous Ubc9, COS-1 cells were transfected with an expression plasmid encoding either FLAG tag or FLAG-SREBP-1a/-2.

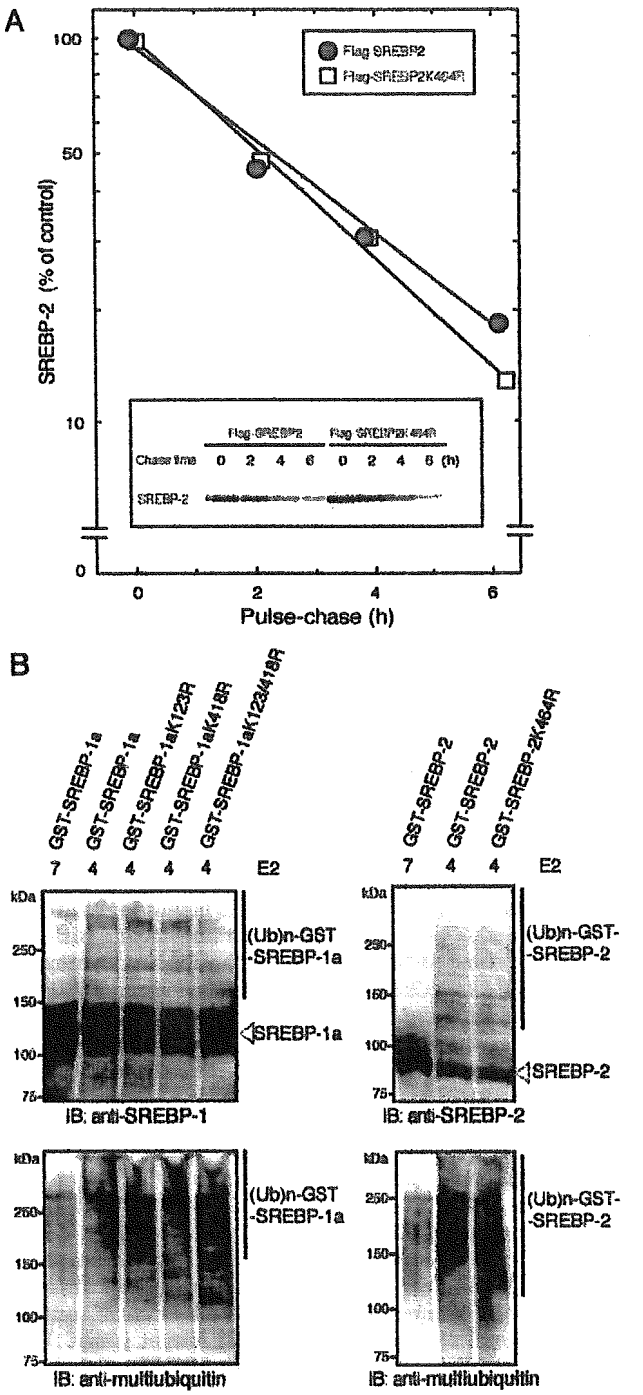

FIG. 6. **Effects of sumoylation of nuclear SREBPs on their stability and ubiquitylation.** *A*, COS-1 cells were transfected with an expression plasmid encoding either wild-type or K464R SREBP-2. After a 24-h incubation, the cells were trypsinized and reseeded in 60-mm plates to normalize the transfection efficiency. After further incubation for 24 h, pulse-chase experiments were performed as described under "Experimental Procedures." At the indicated time points, the cell lysates were subjected to immunoprecipitation with anti-FLAG antibodies. All precipitates were fractionated with SDS-PAGE and visualized by autoradiography. The same results were obtained in three separate experiments. *B*, COS-1 cells were transfected with an expression plasmid encoding either wild-type or mutant versions of SREBPs. The purified GST-SREBPs from the cells were subjected to an *in vitro* ubiquitylation assay, as described under "Experimental Procedures." Ubiquitin-modified SREBPs were detected by immunoblotting (*IB*) with anti-SREBP-1/2 (*top*) and multiubiquitin (*bottom*) antibodies. The mobilities of the ubiquitylated and unmodified SREBPs are indicated on the *right*.

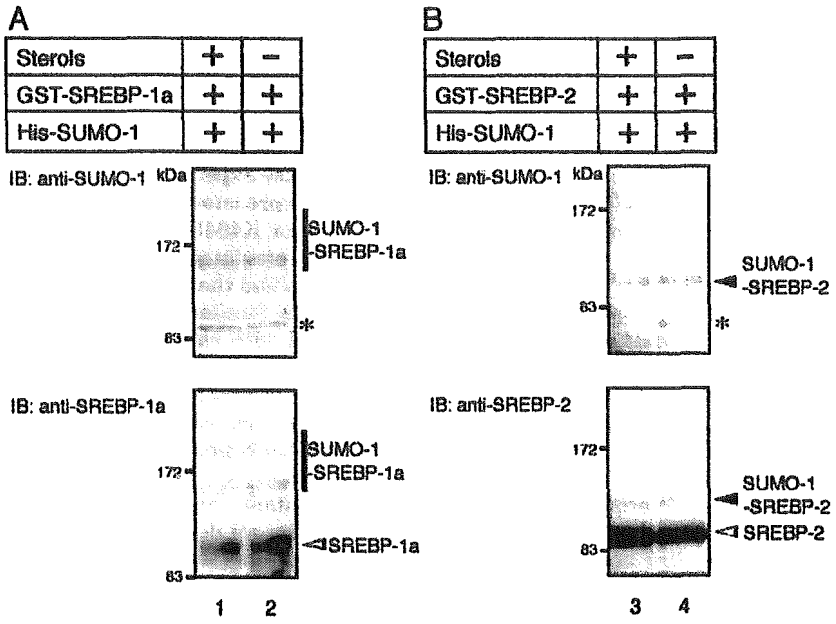

FIG. 7. **Effects of sterols on sumoylation of SREBPs.** M19 cells were co-transfected with expression plasmids encoding His-SUMO-1 and either GST-SREBP-1a (*A*) or -2 (*B*), and then cultured under either sterol-loaded (*lanes 1* and *3*) or sterol-depleted (*lanes 2* and *4*) conditions. GST-SREBPs bound to glutathione-Sepharose resins were subjected to immunoblotting (*IB*) with anti-SUMO-1 (*top*) and SREBP-1/2 (*bottom*) antibodies. The mobilities of the SUMO-1-modified and -unmodified SREBPs are indicated on the *right*. The positions of molecular mass standards are marked on the *left*. The *asterisks* mark the nonspecific bands observed in all lanes.

The supernatants of cell lysates were subjected to immunoprecipitation with anti-FLAG antibodies and visualized by immunoblotting with anti-Ubc9 (Fig. 8*A*, *middle*) and SREBP-1/2 (*top*) antibodies. Ubc9 was co-immunoprecipitated with FLAG-SREBPs (*lanes 2* and *4*), indicating that Ubc9 is capable of interacting with the SREBPs. To further investigate whether Ubc9 catalyzes sumoylation of SREBPs, COS-1 cells were transiently transfected with expression plasmids for GST-SREBPs, His-SUMO-1, and either GFP or GFP-Ubc9(C93S), a dominant negative form of Ubc9 (44). GST-SREBPs bound to glutathione-Sepharose resins were subjected to immunoblotting with anti-SUMO-1 (*top*) and SREBP-1/2 (*middle*) antibodies. Overexpression of GFP-Ubc9(C93S) inhibited sumoylation of SREBPs (Fig. 8*B*, *lanes 6* (*solid bar*) and *8* (*solid arrowhead*)). Thus, we conclude that the dominant negative form of Ubc9 competes with the endogenous one, resulting in decreased modification of the nuclear SREBPs.

To examine whether the dominant negative form of Ubc9 is capable of repressing sumoylation of endogenous SREBPs, thereby enhancing the transcriptional activities, HeLa cells were transfected with an expression plasmid for Ubc9(C93S). Northern blots of SREBP-responsive genes shown in Fig. 8*C* indicate that overexpression of Ubc9(C93S) increased the amounts of HMG-CoA synthase and LDL receptor mRNA in a dose-dependent manner, indicating that blockade of sumoylation accelerated transcription of SREBP target genes. These results suggest that Ubc9 interacts with SREBPs, thereby enhancing the attachment of SUMO-1 to SREBPs and suppressing their transcriptional activities.

DISCUSSION

The aim of this study was to identify posttranslational modification of the SREBPs other than ubiquitylation and to elucidate the mechanisms that modulate SREBP activities through such modifications. The major findings of the present study were 1) SUMO-1 modifies nuclear SREBPs in a Ubc9-dependent manner, 2) residues Lys^{123} and Lys^{418} of SREBP-1a and Lys^{464} of SREBP-2 can act as potential SUMO-1 acceptor sites, and 3) SUMO-1 can negatively regulate the transactivation function of SREBPs. These sumoylation motifs are all conserved in vertebrate SREBPs whose sequences have been so far reported (U00968 for human, U09103 for Chinese hamster, AF286470 for rat, and AY029224 for chicken SREBP-1; U02031 for human, U12330 for Chinese hamster, and AJ414379 for chicken SREBP-2).

Mutation analysis revealed that residues both Lys^{123} and Lys^{418} are required for a full repression of the SREBP-1a transcriptional activity, whereas Lys^{464} is sufficient for a full repression of SREBP-2 to an extent comparable with that elicited by double mutation in SREBP-1a (Fig. 5). It remains unknown why SREBP-1a needs two sumoylation sites to control its transactivation function. Interestingly, the amino acid sequence surrounding Lys^{123} in SREBP-1a, PGIK^{123}EESVP, perfectly conforms to the consensus sequence, PX0–4(I/V)K(Q/T/S/L/E/P)EX0–3P, identified recently in the negative regulatory domain of several transcription factors and named the synergy control (SC) motif (45). The putative SC/sumoylation sites in androgen receptor, glucocorticoid receptor, and c-Myb were found to be functional (31, 32, 46). It is hypothesized that an as yet unidentified SC factor might be recruited to the SC motifs, thereby limiting the transcriptional activities of certain transcription factors. The current finding that covalent attachment of SUMO-1 at Lys^{123} in the SC motif attenuates the transactivation function of SREBP-1a implies involvement of such SC factor in a sumoylation-dependent manner. However, whether the hypothetical SC factor recognizes unmodified SC motifs or sumoylated motifs remains obscure, because sumoylation of the SC motifs in SREBP-1a as well as androgen receptor and c-Myb attenuates their transactivation capacity, whereas sumoylation of glucocorticoid receptor elicits the opposite effect.

We found that the C-terminal domain containing ~90 amino acids of the nuclear SREBPs exerts a transcriptional repression function when fused to the Gal4 DNA binding domain plus the SREBP-1a activation domain containing the N-terminal 50 amino acids (data not shown). In a previous study, we indeed noticed that truncation of the domain in a nuclear form of SREBP-1 somehow potentiated the transcriptional activities (2). The residues Lys^{418} of SREBP-1a and Lys^{464} of SREBP-2 are located in this negative regulatory domain and are likely to be involved in such repression. The amino acid sequence surrounding Lys^{464} in SREBP-2, VK^{464}DEP, matches the consensus sumoylation site found in the negative regulatory domain of four CCAAT/enhancer-binding protein family members, which is evolutionally conserved in a variety of vertebrate species (47). However, SUMO-1 attachment augmented the

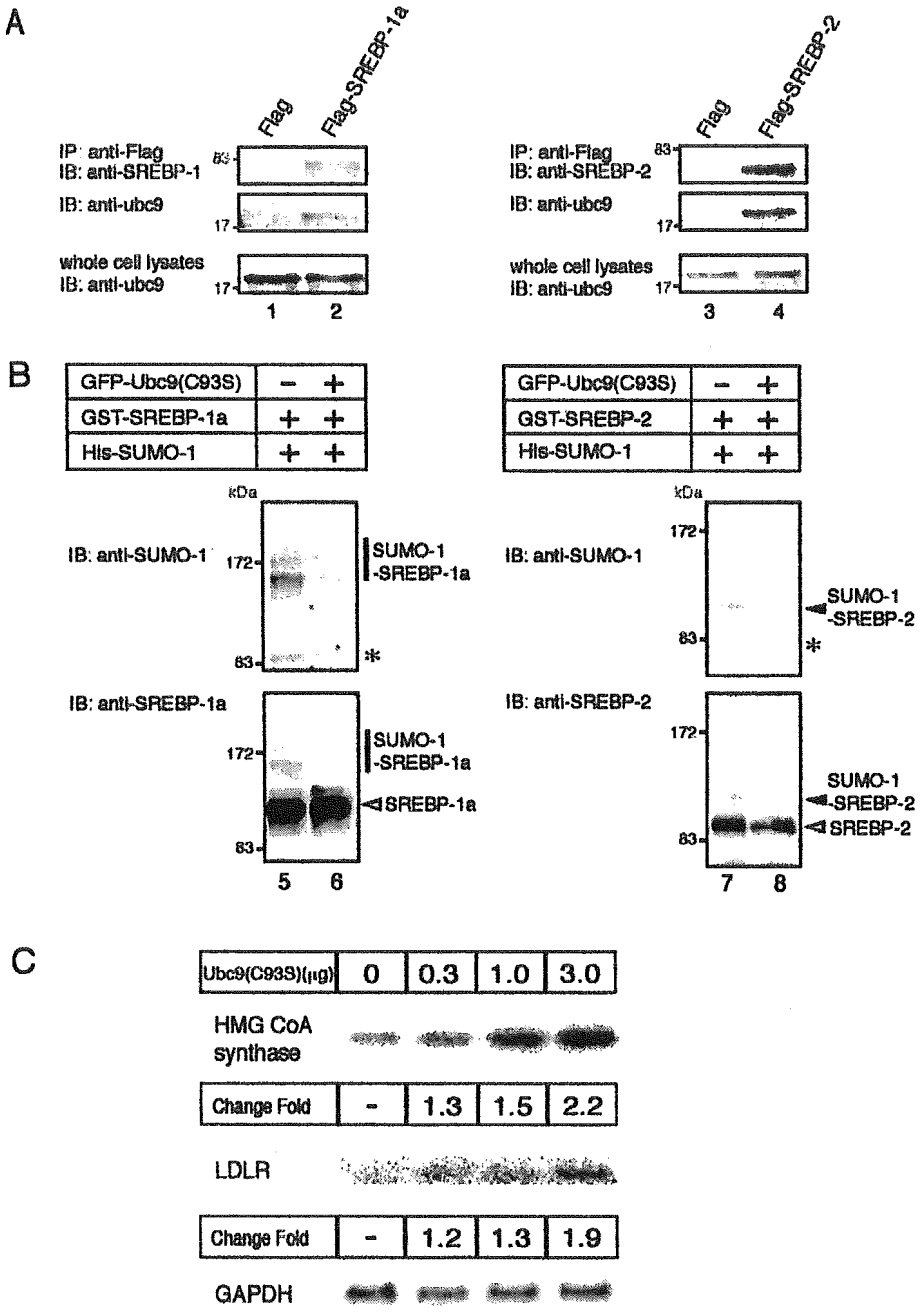

FIG. 8. **Ubc9 interacts with SREBPs and catalyzes attachment of SUMO-1 to SREBPs.** *A*, COS-1 cells were transfected with an expression plasmid encoding either FLAG tag (*lanes 1* and *3*) or FLAG-SREBPs (*lanes 2* and *4*). The cell lysates were subjected to immunoprecipitation (*IP*) with anti-FLAG antibodies and immunoblotting (*IB*) with anti-SREBP-1/2 (*top*) and Ubc9 (*middle*) antibodies. Expression of endogenous Ubc9 was evaluated by immunoblotting in normalized whole cell lysates (10 μg/lane) using anti-Ubc9 antibodies (*bottom*). *B*, COS-1 cells were cotransfected with expression plasmids for GST-SREBPs, His-SUMO-1, and either GFP (*lanes 5* and *7*) or GFP-Ubc9 (C93S) (*lanes 6* and *8*). GST-SREBPs bound to glutathione-Sepharose resins were subjected to immunoblotting (*IB*) with anti-SUMO-1 (*top*) and SREBP-1/2 (*bottom*). The *asterisks* mark the nonspecific bands observed in all lanes. *C*, HeLa cells in a 60-mm dish were transfected with the indicated amounts of expression plasmid for His-Ubc9(C93S). After transfection, the cells were cultured under sterol-depleted conditions for 48 h. Total RNA (8 μg/lane) was subjected to Northern blot analysis as described in the legend to Fig. 2. The same results were obtained in three separate experiments.

inhibitory effect of the SREBP-2-negative regulatory domain but decreased that of the CCAAT/enhancer-binding protein regulatory domain. In the case of SREBPs, covalent conjugation of SUMO-1 to Lys^{418} or Lys^{464} could potentially influence the flexibility of the C terminus as observed in sumoylated RanGAP1 (21). In support of this notion, the different migration patterns of the sumoylated bands modified at Lys^{123} and Lys^{418} in SREBP-1a (Fig. 3) suggest that sumoylation of SREBPs might induce conformational changes in these proteins.

Sumoylation has been shown to be responsible for the translocation of some proteins into discrete subnuclear matrix-associated structures, called the promonocytic leukemia nuclear bodies (23, 48). Several proteins, including Sp100, Daxx, CCAAT/enhancer-binding protein, and ISG20, have been reported to be targeted to the nuclear bodies after SUMO-1 modification (19); however, this does not necessarily mean that all SUMO-1-conjugated proteins are destined to be localized in the nuclear body (49). Interestingly, although the biological function of the nuclear body is unclear, it has been recently shown that sumoylation directly or indirectly promotes promonocytic leukemia degradation (50). Although we examined whether mutations in the SUMO-1 sites affect the intracellular localization of the GFP-tagged SREBPs, sumoylation did not induce significant changes in the distribution of them in the nucleus (data not shown). Further studies are required to investigate the role of SUMO-1 modification of several target proteins including SREBPs on their subnuclear localization in order to understand the biological functions of sumoylation.

Figs. 1, 3, and 4 show that the sumoylated SREBPs were barely detected compared with unmodified SREBPs in these

experiments. This does not appear to be in line with the results of transactivation experiments shown in Fig. 5, in which mutations in the SUMO-1 acceptor sites resulted in marked increases of the transcriptional activities of SREBPs, and the findings that expression of SREBP-responsive genes was diminished by overexpression of SUMO-1 but increased by overexpression of dominant negative SUMO-1 (Fig. 2). Sumoylated proteins are considered as very transient structures resulting from a dynamic equilibrium between SUMO-1-conjugated and -deconjugated forms (51). Thus, sumoylation is likely to represent a mechanism for rapid and reversible control, and target proteins are conjugated during a short period of time, which is nevertheless sufficient to affect their biological activities. So far, a number of mammalian desumoylating enzymes, which remove SUMO-1 from its protein conjugates, have been identified (19). The different patterns of subcellular or tissue distribution of these enzymes may reflect the specific function of each enzyme at its location and suggest that desumoylation, like deubiquitylation, plays an important role in regulation of SUMO-1-mediated cellular processes.

The biological consequences of sumoylation and ubiquitylation are quite different despite the facts that both SUMO-1 and ubiquitin are conjugated to a lysine residue in target proteins and that their modification machineries are mechanistically very similar. The addition of a polyubiquitin chain to a lysine residue marks modified proteins for a rapid degradation by the 26 S proteasome. In contrast, sumoylation has been shown to increase the stability of IκBα by antagonizing ubiquitylation (24). We previously reported that nuclear SREBPs are degraded through the ubiquitin/26 S proteasome pathway (8). In the present study, we provided experimental evidence that SUMO-1 modification of the SREBPs could not alter their stability (Fig. 6*A*) and that SUMO-1 conjugation did not compete with ubiquitin modification (Fig. 6*B*). We devised a unique *in vitro* ubiquitylation assay, in which ubiquitin conjugation occurred without the addition of a specific E3 ligase for SREBPs in the presence of recombinant E1 and E2. It is likely that the GST-SREBPs prepared from cells treated with a proteasome inhibitor trapped an unidentified functional E3 ligase, which was capable of attaching ubiquitin to the SREBPs. Based on these results, we conclude that lysine residues of sumoylation sites in the SREBPs are at least not the major potential ubiquitylation sites. Taken together, the independence of these two processes implies that inactivation of SREBPs is doubly regulated by sumoylation and by their destruction through the ubiquitin/26 S proteasome pathway. These results also support the notion that the two independent processes might be required for sufficient elimination of unexpected increases in the expression of the SREBP-responsive genes to maintain homeostasis of lipid metabolism.

SREBPs are synthesized as membrane-bound precursors and activated by a proteolytic process regulated by intracellular sterol levels. In addition to the proteolytic processing, a rise in intracellular sterol levels, probably cholesterol levels in nuclear membranes, might accelerate the rate of SUMO-1 conjugation to the nuclear SREBPs, which in turn negatively regulates their transactivation function to suppress the expression of genes encoding enzymes for cholesterol biosynthesis. However, the results shown in Fig. 7 clearly rule out this hypothesis. In a previous study, we also demonstrated that intracellular sterol levels do not alter the rapid degradation of nuclear SREBPs through the ubiquitin/26 S proteasome pathway (8). Taken together, these studies suggest that two independent processes, ubiquitin-dependent degradation and SUMO-1-mediated inactivation, are not regulated in response to changes in lipid metabolism but act constitutively to control the transcriptional activities of the nuclear SREBPs.

In conclusion, the importance of SUMO-1 modification for modulating the transactivation function of nuclear SREBPs is now emerging. Our work reports a new mechanism through which sumoylation can exert its negative effect on SREBPs function and govern lipid metabolism.

Acknowledgments—We thank Tomoki Chiba (Tokyo Metropolitan Institute of Medical Science) and Minoru Yoshida for the helpful comments and discussions. We are grateful to Tohru Tezuka for kindly providing the GST expression plasmids.

REFERENCES

1. Brown, M. S., and Goldstein, J. L. (1999) *Proc. Natl. Acad. Sci. U. S. A.* **96,** 11041–11048
2. Sato, R., Yang, J., Wang, X., Evans, M. J., Ho, Y. K., Goldstein, J. L., and Brown, M. S. (1994) *J. Biol. Chem.* **269,** 17267–17273
3. Wang, X., Sato, R., Brown, M. S., Hua, X., and Goldstein, J. L. (1994) *Cell* **77,** 53–62
4. Sakai, J., Duncan, E. A., Rawson, R. B., Hua, X., Brown, M. S., and Goldstein, J. L. (1996) *Cell* **85,** 1037–1046
5. Hua, X., Nohturfft, A., Goldstein, J. L., and Brown, M. S. (1996) *Cell* **87,** 415–426
6. Espenshade, P. J., Cheng, D., Goldstein, J. L., and Brown, M. S. (1999) *J. Biol. Chem.* **274,** 22795–22804
7. Nagoshi, E., Imamoto, N., Sato, R., and Yoneda, Y. (1999) *Mol. Biol. Cell* **10,** 2221–2233
8. Hirano, Y., Yoshida, M., Shimizu, M., and Sato, R. (2001) *J. Biol. Chem.* **276,** 36431–36437
9. Jin, C., Shiyanova, T., Shen, Z., and Liao, X. (2001) *Int. J. Biol. Macromol.* **28,** 227–234
10. Yeh, E. T., Gong, L., and Kamitani, T. (2000) *Gene (Amst.)* **248,** 1–14
11. Hochstrasser, M. (2001) *Cell* **107,** 5–8
12. Varshavsky, A. (1997) *Trends Biochem. Sci.* **22,** 383–387
13. Saitoh, H., Pu, R. T., and Dasso, M. (1997) *Trends. Biochem. Sci.* **22,** 374–376
14. Johnson, E. S., Schwienhorst, I., Dohmen, R. J., and Blobel, G. (1997) *EMBO J.* **16,** 5509–5519
15. Johnson, E. S., and Blobel, G. (1997) *J. Biol. Chem.* **272,** 26799–26802
16. Desterro, J. M., Thomson, J., and Hay, R. T. (1997) *FEBS Lett.* **417,** 297–300
17. Sampson, D. A., Wang, M., and Matunis, M. J. (2001) *J. Biol. Chem.* **276,** 21664–21669
18. Bernier-Villamor, V., Sampson, D. A., Matunis, M. J., and Lima, C. D. (2002) *Cell* **108,** 345–356
19. Kim, K. I., Baek, S. H., and Chung, C. H. (2002) *J. Cell. Physiol.* **191,** 257–268
20. Muller, S., Hoege, C., Pyrowolakis, G., and Jentsch, S. (2001) *Nat. Rev. Mol. Cell. Biol.* **2,** 202–210
21. Mahajan, R., Delphin, C., Guan, T., Gerace, L., and Melchior, F. (1997) *Cell* **88,** 97–107
22. Seeler, J. S., Marchio, A., Losson, R., Desterro, J. M., Hay, R. T., Chambon, P., and Dejean, A. (2001) *Mol. Cell. Biol.* **21,** 3314–3324
23. Zhong, S., Muller, S., Ronchetti, S., Freemont, P. S., Dejean, A., and Pandolfi, P. P. (2000) *Blood* **95,** 2748–2752
24. Desterro, J. M., Rodgriguez, M. S., and Hay, R. T. (1998) *Mol. Cell,* **2,** 233–239
25. Hoege, C., Pfander, B., Moldovan, G. L., Pyrowolakis, G., and Jentsch, S. (2002) *Nature* **419,** 135–141
26. Fogal, V., Gostissa, M., Sandy, P., Zacchi, P., Sternsdorf, T., Jensen, K., Pandolfi, P. P., Will, H., Schneider, C., and Del Sal, G. (2000) *EMBO J.* **19,** 6185–6195
27. Goodson, M. L., Hong, Y., Rogers, R., Matunis, M. J., Park-Sarge, O. K., and Sarge, K. D. (2001) *J. Biol. Chem.* **276,** 18513–18518
28. Hong, Y., Rogers, R., Matunis, M. J., Mayhew, C. N., Goodson, M. L., Park-Sarge, O. K., and Sarge, K. D. (2001) *J. Biol. Chem.* **276,** 40263–40267
29. Minty, A., Dumont, X., Kaghad, M., and Caput, D. (2000) *J. Biol. Chem.* **275,** 36316–36323
30. Muller, S., Berger, M., Lehembre, F., Seeler, J. S., Haupt, Y., and Dejean, A. (2000) *J. Biol. Chem.* **275,** 13321–13329
31. Poukka, H., Karvonen, U., Janne, O. A., and Palvimo, J. J. (2000) *Proc. Natl. Acad. Sci. U. S. A.* **97,** 14145–14150
32. Bies, J., Markus, J., and Wolff, L. (2002) *J. Biol. Chem.* **277,** 8999–9009
33. Inoue, J., Sato, R., and Maeda, M. (1998) *J. Biochem. (Tokyo)* **123,** 1191–1198
34. Sato, R., Okamoto, A., Inoue, J., Miyamoto, W., Sakai, Y., Emoto, N., Shimano, H., and Maeda, M. (2000) *J. Biol. Chem.* **275,** 12497–12502
35. Sato, R., Miyamoto, W., Inoue, J., Terada, T., Imanaka, T., and Maeda, M. (1999) *J. Biol. Chem.* **274,** 24714–24720
36. Nakahara, M., Fujii, H., Maloney, P. R., Shimizu, M., and Sato, R. (2002) *J. Biol. Chem.* **277,** 37229–37234
37. Inoue, J., Kumagai, H., Terada, T., Maeda, M., Shimizu, M., and Sato, R. (2001) *Biochem. Biophys. Res. Commun.* **283,** 1157–1161
38. Sato, R., Inoue, J., Kawabe, Y., Kodama, T., Takano, T., and Maeda, M. (1996) *J. Biol. Chem.* **271,** 26461–26464
39. Murata, S., Minami, Y., Minami, M., Chiba, T., and Tanaka, K. (2001) *EMBO Rep.* **21,** 1133–1138
40. Tatham, M. H., Jaffray, E., Vaughan, O. A., Desterro, J. M., Botting, C. H., Naismith, J. H., and Hay, R. T. (2001) *J. Biol. Chem.* **276,** 35368–35374
41. Osborne, T. F. (2000) *J. Biol. Chem.* **275,** 32379–32382
42. Kamitani, T., Nguyen, H. P., and Yeh, E. T. H. (1997) *J. Biol. Chem.* **272,**

14001–14004
43. Rawson, R. B., Zelenski, N. G., Nijihawan, D., Ye, J., Sakai, J., Hasan, M. T., Chang, T. Y., Brown, M. S., and Goldstein, J. L. (1997) *Mol. Cell* **1,** 47–57
44. Gong, L., Kamitani, T., Fujise, K., Caskey, L. S., and Yeh, E. T. (1997) *J. Biol. Chem.* **272,** 28198–28201
45. Iniguez-Lluhi, J. A., and Pearce, D. (2000) *Mol. Cell. Biol.* **20,** 6040–6050
46. Drean, Y. L., Mincheneau, N., Goff, P. L., and Michel, D. (2002) *Endocrinology* **143,** 3482–3489
47. Kim, J., Cantwell, C. A., Johnson, P. F., Pfarr, C. M., and Williams, S. C. (2002) *J. Biol. Chem.* **277,** 38037–38044
48. Sternsdorf, T., Jensen, K., and Will, H. (1997) *J. Cell Biol.* **139,** 1621–1634
49. Kirsh, O., Seeler, J. S., Pichler, A., Gast, A., Muller, S., Miska, E., Mathieu, M., Harel-Bellan, A., Kouzarides, T., Melchior, F., and Dejean, A. (2002) *EMBO J.* **21,** 2682–2691
50. Mattsson, K., Pokrovskaja, K., Kiss, C., Klein, G., and Szekely, L. (2001) *Proc. Natl. Acad. Sci. U. S. A.* **98,** 1012–1017
51. Schwienhorst, I., Johnson, E. S., and Dohmen, R. J. (2000) *Mol. Gen. Genet.* **263,** 771–786

Insulin-induced phosphorylation of FKHR (Foxo1) targets to proteasomal degradation

Hitomi Matsuzaki*, Hiroaki Daitoku*, Mitsutoki Hatta*†, Keiji Tanaka‡, and Akiyoshi Fukamizu*§

*Center for Tsukuba Advanced Research Alliance, Institute of Applied Biochemistry, University of Tsukuba, Tsukuba, Ibaraki 305-8577, Japan; †Department of Oral Pathobiology, Hokkaido University, Sapporo 060-8586, Japan; and ‡Department of Molecular Oncology, Tokyo Metropolitan Institute of Medical Science, Bunkyo-ku, Tokyo 113-8613, Japan

Edited by Bruce M. Spiegelman, Harvard Medical School, Boston, MA, and approved July 31, 2003 (received for review July 6, 2003)

Forkhead transcription factor FKHR (Foxo1) is a key regulator of glucose homeostasis, cell-cycle progression, and apoptosis. It has been shown that FKHR is phosphorylated via insulin or growth factor signaling cascades, resulting in its cytoplasmic retention and the repression of target gene expression. Here, we investigate the fate of FKHR after cells are stimulated by insulin. We show that insulin treatment decreases endogenous FKHR proteins in HepG2 cells, which is inhibited by proteasome inhibitors. FKHR is ubiquitinated *in vivo* and *in vitro*, and insulin enhances the ubiquitination in the cells. In addition, the signal to FKHR degradation from insulin is mediated by the phosphatidylinositol 3-kinase pathway, and the mutation of FKHR at the serine or threonine residues phosphorylated by protein kinase B, a downstream target of phosphatidylinositol 3-kinase, inhibits the ubiquitination *in vivo* and *in vitro*. Finally, efficient ubiquitination of FKHR requires both phosphorylation and cytoplasmic retention in the cells. These results demonstrate that the insulin-induced phosphorylation of FKHR leads to the multistep negative regulation, not only by the nuclear exclusion but also the ubiquitination-mediated degradation.

Protein kinase B (PKB, also called Akt) plays a critical role in mediating various effects of insulin and related growth factors, downstream from phosphatidylinositol 3-kinase (PI3K) (1, 2). PKB promotes cell survival and proliferation and regulates metabolic homeostasis in part by modulating transcriptional activity of the FOXO subfamily of Forkhead transcription factors, including FKHR (Foxo1), FKHRL1 (Foxo3a), and AFX (Foxo4), through phosphorylation (3, 4). In the absence of phosphorylation, these FOXO transcription factors localize in the nucleus and interact with the insulin response sequences within the promoters of multiple target genes. Once bound to the target gene promoters via insulin response sequences, the FOXOs act as a potent activator of transcription. On the other hand, when PKB is activated by insulin, the FOXO proteins are directly phosphorylated, resulting in their nuclear export and cytoplasmic retention through the binding to 14-3-3 proteins and the inhibition of target gene expression (5–9).

Recent studies have revealed that FOXOs are implicated in modulating various cellular activities in different cell types. For instance, in hepatocytes, FOXOs regulate the transcription of gluconeogenic key factors, including glucose-6-phosphatase, phosphoenolpyruvate carboxykinase, and peroxisome proliferator-activated receptor-γ coactivator-1 (10–13). Nakae *et al.* (14) have also reported recently that FKHR (Foxo1) controls hepatic glucose production and β cell compensation for insulin resistance in type 2 diabetes by the genetic analysis with the gain- and loss-of-functions of FKHR alleles in mice. In *Caenorhabditis elegans*, several studies have provided genetic evidence that FOXO homologue Daf-16 acts as a determinant of longevity, probably by inducing several stress-resistance genes (15–17). More recent studies demonstrated that FOXOs regulate the gene expression of catalase and manganese superoxide dismutase, which protect cells against oxidative stress (18, 19), and suggested that FOXOs are able to control lifespan in mammals. In addition, it has been shown that FOXOs can mediate the transcriptional activity of nuclear hormone receptors by serving as either a coactivator or a corepressor (20–22).

The relevance of the FOXO family to diverse physiological events in the transcription-based function is of significant interest. In postphosphorylation, however, the fate of FOXO proteins remains to be explored. Here, we show that FKHR (Foxo1) is a substrate of insulin-dependent polyubiquitination and degradation. Significantly, FKHR 3A mutant, resistant to PKB phosphorylation, was unable to be polyubiquitinated *in vivo* and *in vitro*, suggesting the requirement of the "phosphorylated" state for ubiquitination. Furthermore, the cytoplasmic retention in addition to phosphorylation achieves the effective ubiquitination of FKHR. Taken together, our results provide evidence for the mechanism whereby insulin signaling leads to FKHR polyubiquitination, resulting in down-regulation of the protein level via proteasome-dependent degradation.

Materials and Methods

Cell Culture and Western Blot Analysis. HepG2 and HEK293T cells were cultured in DMEM supplemented with 10% FBS. Before the insulin treatment of HepG2 cells, medium was replaced with serum-free DMEM containing 0.1% BSA and incubated for 12 h, and then added with insulin (100 nM) with or without proteasome inhibitors (10 μM MG132, 10 μM lactacystin, or 10 μM epoxomicin). In some experiments, cells were pretreated with LY294002 (20 μM) or wortmannin (100 nM) for 30 min before insulin stimulation. After washing with PBS, cells were lysed with lysis buffer (50 mM Tris·HCl, pH 7.5/150 mM NaCl/1% Triton X-100/0.1% SDS/0.5% sodium deoxycholate/10% glycerol/5 mM NaF/1 mM sodium orthovanadate and protease inhibitors). Forty micrograms of whole cell extracts were resolved by SDS/PAGE, followed by electrotransfer onto poly(vinylidene difluoride) membranes and probing with an anti-FKHR antibody. Chemiluminescent detection relied on horseradish peroxidase-conjugated secondary antibodies.

Antibodies. A rabbit polyclonal antibody specific for mouse FKHR was raised against the bacterially expressed GST-FKHR (541–652 aa) fusion protein as described (13). Anti-FLAG (M2) and anti-β-actin (AC-74) were purchased from Sigma. Anti-hemagglutinin (anti-HA) (3F10) was obtained from Roche Molecular Biochemicals. Anti-phospho-PKB/Akt (Ser-473), anti-PKB/Akt, and anti-phospho-FKHR (Ser-256) were from Cell Signaling Technology (Beverly, MA). Anti-Xpress was from Invitrogen.

Cloning and Plasmids. pcDNA3-FLAG-FKHR was generated by RT-PCR-based cloning of mouse FKHR cDNA into pcDNA3-

This paper was submitted directly (Track II) to the PNAS office.

Abbreviations: PKB, protein kinase B; PI3K, phosphatidylinositol 3-kinase; NLS, nuclear localization signal; NES, nuclear export signal; HA, hemagglutinin; RRL, rabbit reticulocyte lysate.

§To whom correspondence should be addressed. E-mail: akif@tara.tsukuba.ac.jp.

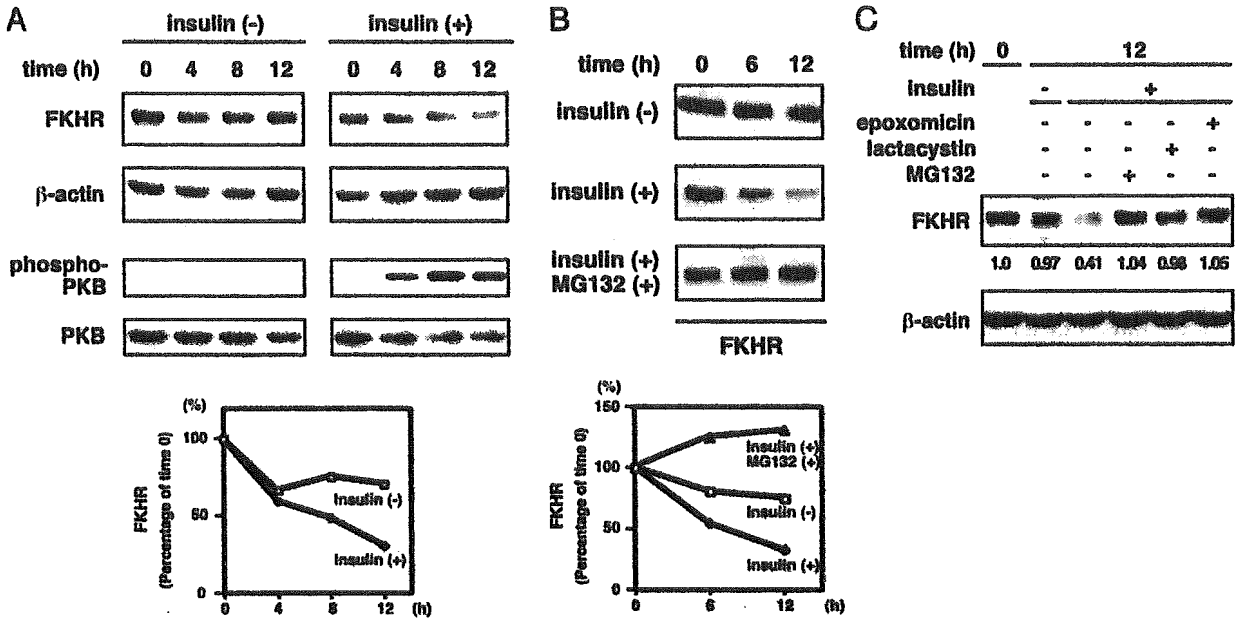

Fig. 1. Insulin induces FKHR turnover through proteasomal degradation. (*A* and *B*) HepG2 cells were serum-starved for 12 h and treated with 100 nM insulin (*A*), with or without a proteasome inhibitor MG132 (*B*), for the indicated periods. Whole cell extracts were analyzed by immunoblotting. (*C*) HepG2 cells were serum-starved for 12 h and treated with insulin in the presence or absence of indicated proteasome inhibitors for 12 h. Whole cell extracts were analyzed by immunoblotting.

FLAG vector as described (23). The putative PKB phosphorylation sites at Thr-24, Ser-253, and Ser-316 of FKHR were mutated to alanines by PCR mutagenesis. The critical residues in nuclear localization signal (NLS) or nuclear export signal (NES) of FKHR were also mutated to alanines by PCR mutagenesis. pcDNA3-HA-ubiquitin was described (24). GST-HA-ubiquitin was made by PCR-based subcloning into pGEX-4T vector (Amersham Pharmacia). cDNA of Δp85, which is p85 subunit of PI3K lacking binding site for its catalytic p110 subunit (25), was kindly provided by W. Ogawa (Kobe University, Kobe, Japan) and was subcloned into pcDNA3.1-HisC vector (Invitrogen) to express Xpress epitope-tagged Δp85 (Xp-Δp85).

Immunoprecipitation. To detect the ubiquitination of FKHR *in vivo*, HepG2 cells were transfected with FLAG-FKHR and HA-ubiquitin expression plasmids by using FuGENE 6 reagents (Roche Molecular Biochemicals). Thirty-six hours after transfection, cells were treated with MG132, lactacystin, or epoxomicin for 12 h, then lysed in lysis buffer. Where indicated, before treatment with insulin and MG132, cells were serum-starved for 12 h. Whole cell extracts were subjected to immunoprecipitation with anti-FLAG antibody. To test whether FKHR is covalently linked to ubiquitin, immunoprecipitates were eluted from the beads by heating in the presence of 1% SDS and reimmunoprecipitated with the same antibody as described (26). All of the immune complexes were resolved by SDS/PAGE, followed by Western blot analysis.

***In Vitro* Ubiquitination Assay.** The *in vitro* ubiquitination assay was performed as described (27) with minor modifications. HEK293T cells were transfected with FLAG-FKHR wild-type or T24A/S253A/S316A (3A) mutant as described above. Forty-eight hours later, cells were lysed in lysis buffer, and whole cell extracts were subjected to immunoprecipitation with anti-FLAG antibody. The immune complexes were washed with lysis buffer, followed with reaction buffer. The reaction mixture contained the immunoprecipitates, 50 mM Tris·HCl (pH 7.5), 10 mM $MgCl_2$, 0.5 mM DTT, ATP regenerating system (2 mM ATP, 10 mM creatine phosphate, 10 units/ml creatine kinase, and 1 unit/ml inorganic pyrophosphatase), 20 μM MG132, and 33% (vol/vol) crude rabbit reticulocyte lysate (RRL, Promega), with 6 μg of bacterially expressed GST, GST-HA-ubiquitin, or 3 μg of ubiquitin (Sigma). After incubation at 30°C for 1 h, the beads were extensively washed with reaction buffer containing 1% Triton X-100. In some cases, the reaction products were eluted with FLAG peptide (Sigma), and ubiquitinated FKHR was purified with glutathione-Sepharose beads (Amersham Pharmacia) or an anti-HA antibody. All of the reaction products were analyzed by Western blotting.

Immunofluorescence. HepG2 cells were plated onto glass coverslips and transfected by using FuGENE 6 reagents. Forty-eight hours after transfection, cells were fixed with 3.7% paraformaldehyde in PBS for 20 min and permeabilized by treatment with 0.1% Triton X-100 in PBS for 30 min. After blocking with 3% BSA, 0.1% Tween 20 in PBS for 1 h, cells were incubated with anti-FLAG antibody, followed by staining with Alexa Fluor 488 anti-mouse secondary antibody (Molecular Probes).

Results

Down-Regulation of FKHR Expression by Insulin. To explore the fate of FKHR subsequent to phosphorylation and cytoplasmic retention in response to insulin, we first examined the kinetics of FKHR stability after the stimulation. Serum-starved HepG2 cells were cultured in the presence or absence of insulin, and cell extracts were harvested at different time points after the stimulation to monitor the amount of endogenous FKHR by using anti-FKHR antibody. Interestingly, although little change in stability was observed in the untreated cells, insulin stimulation decreased the level of FKHR protein in a time-dependent manner (Fig. 1*A*). At the same time, PKB was activated by insulin stimulation.

Because it is known that various cellular proteins, including transcription factors, are tightly regulated by proteolysis through proteasome in response to external signaling molecules (28, 29), we next sought to determine whether a proteasome-mediated

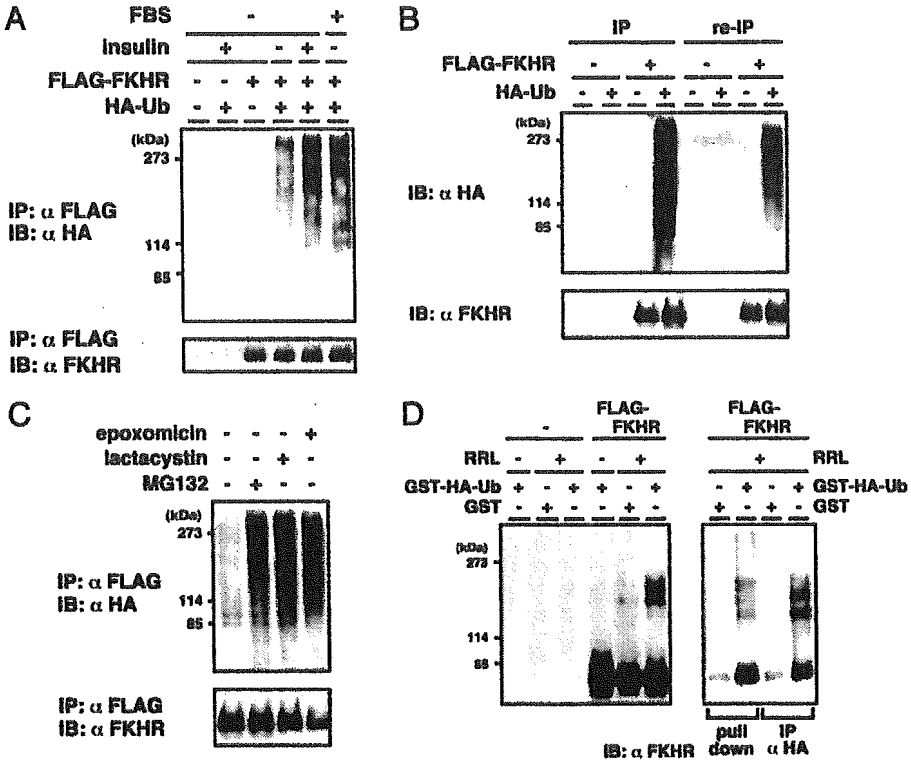

Fig. 2. FKHR is ubiquitinated *in vivo* and *in vitro*. (*A*) HepG2 cells were transfected with the FLAG-FKHR and HA-ubiquitin expression plasmids. Twenty-four hours after transfection, cells were serum-starved for 12 h and incubated with MG132 with or without insulin or FBS for a further 12 h. Whole cell extracts were subjected to anti-FLAG immunoprecipitation (IP) and followed by anti-HA (*Upper*) or anti-FLAG (*Lower*) immunoblotting. (*B*) HepG2 cells were transfected with the FLAG-FKHR and HA-ubiquitin expression plasmids and treated with MG132 for 10 h before cell lysis. Whole cell extracts were subjected to anti-FLAG immunoprecipitation. The immunoprecipitated materials were eluted from the beads by heating in the presence of 1% SDS and reimmunoprecipitated (re-IP) with the same antibody. All of the immune complexes were analyzed as in *A*. (*C*) HepG2 cells transfected with the FLAG-FKHR and HA-ubiquitin were treated with indicated proteasome inhibitors, and ubiquitination was detected as in *A*. (*D*) Cell extracts from HEK293T cells transfected with the FLAG-FKHR plasmid were subjected to anti-FLAG immunoprecipitation. The immune complexes were incubated at 30°C for 1 h with or without RRL and either GST or GST-HA-ubiquitin. (*Right*) The reaction products were eluted by FLAG peptide, again subjected to pull-down by glutathione-Sepharose or to immunoprecipitation by using anti-HA antibody. All of the reaction products were analyzed by immunoblotting with anti-FKHR antibody.

degradation is involved in the insulin-dependent decline of FKHR level. To address this question, serum-starved HepG2 cells were cultured with insulin in the presence or absence of a proteasome inhibitor, MG132. As shown in Fig. 1*B*, the proteasome inhibition resulted in the drastic stabilization of FKHR despite insulin stimulation. Other proteasome-specific inhibitors, lactacystin and epoxomicin, also stabilized FKHR protein (Fig. 1*C*). This finding provided an indication that FKHR is regulated through proteasome-mediated degradation, which is triggered by insulin stimulation.

Ubiquitination of FKHR *in Vivo* and *in Vitro*. Because the 26S proteasome recognizes and degrades proteins that are conjugated with polyubiquitin chains (30), we investigated whether FKHR is ubiquitinated *in vivo*. HepG2 cells were cotransfected with FLAG-tagged FKHR and HA-tagged ubiquitin expression plasmids and serum-starved before insulin and MG132 treatment. FLAG-FKHR was immunoprecipitated from whole cell extracts and subjected to immunoblotting using anti-HA antibody to detect ubiquitin-conjugated FKHR. A ladder of high molecular weight ubiquitinated products was detected when cells were treated with insulin, whereas only slight signal was seen at an immunoprecipitate from untreated cells (Fig. 2*A*), indicating the insulin-dependent polyubiquitination of FKHR. A similar effect to insulin was observed by the addition of FBS (see Fig. 2*A*). Furthermore, to exclude the possibility that other ubiquitinated proteins coimmunoprecipitated with FKHR may be detected, reimmunoprecipitation assay was performed. After the immunoprecipitated complex was boiled in a buffer containing 1% SDS to disrupt all protein–protein interaction, FKHR was immunoprecipitated again and tested for the ubiquitin conjugation. The shifted ladder larger than unmodified FKHR was detected in the reimmunoprecipitation complex, suggesting that FKHR is indeed a target of the ubiquitination in HepG2 cells (Fig. 2*B*). Several proteasome-specific inhibitors were used to confirm that the ubiquitinated FKHR could be degraded by the 26S proteasome. Consistent with MG132 treatment, lactacystin and epoxomicin, but not solvent DMSO, induced the accumulation of ubiquitinated FKHR (Fig. 2*C*), suggesting that ubiquitinated FKHR is a substrate of the 26S proteasome *in vivo*.

Next, to confirm whether ubiquitin chain is directly attached to FKHR molecule, we performed an *in vitro* cell-free assay. FLAG-FKHR was immunoprecipitated from transfected HEK293T cells and incubated with RRL in the presence of ATP regenerating system and bacterially expressed GST-HA-ubiquitin. By immunoblotting with anti-FKHR antibody, the bands of large molecular size were detected (Fig. 2*D Left*), indicating that FKHR was modified, probably by ubiquitination. Furthermore, to verify that FKHR was indeed ubiquitinated in this assay, the reaction products were eluted by FLAG peptide, followed by pull-down with glutathione-Sepharose or by immunoprecipitation with anti-HA antibody. As shown in Fig. 2*D Right*, the bands of high molecular weight proteins were also probed with anti-FKHR antibody, clearly demonstrating that the modified molecules were ubiquitin-conjugated FKHR.

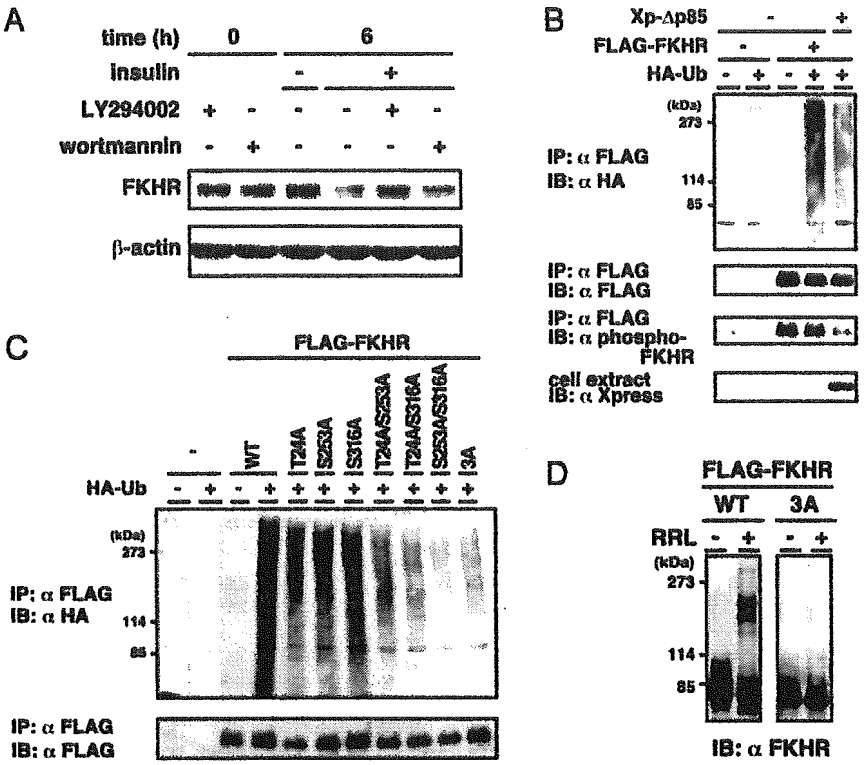

Fig. 3. Phosphorylation via PI3K-PKB pathway is important for FKHR ubiquitination. (*A*) HepG2 cells were serum-starved for 12 h and preincubated with PI3K inhibitor, LY294002, or wortmannin for 30 min and stimulated with insulin for 6 h. Whole cell extracts were analyzed by immunoblotting using anti-FKHR antibody. (*B*) FLAG-FKHR and HA-ubiquitin were cotransfected with a dominant negative mutant of PI3K (Xp-Δp85) expression plasmids in HepG2 cells. After treatment with MG132, whole cell extracts were subjected to anti-FLAG immunoprecipitation and followed by immunoblotting. The expression of Xpress-tagged Δp85 in the cell extract was shown by immunoblotting with anti-Xpress antibody. (*C*) HepG2 cells were transfected with the indicated FKHR mutant and HA-ubiquitin expression plasmids and treated with MG132. Whole cell extracts were subjected to anti-FLAG immunoprecipitation, followed by anti-HA (*Upper*) or anti-FLAG (*Lower*) immunoblotting. (*D*) Cell extracts from HEK293T cells transfected with the FLAG-FKHR WT or 3A plasmid were subjected to anti-FLAG immunoprecipitation. The immune complexes were incubated at 30°C for 1 h in the presence or absence of RRL. The reaction products were analyzed by immunoblotting with anti-FKHR antibody.

Phosphorylation-Dependent Ubiquitination and Degradation of FKHR. Our initial finding of a strong correlation between insulin signaling and FKHR instability prompted us to investigate whether the PI3K-PKB pathway is involved in the signaling for FKHR degradation. To this end, HepG2 cells were preincubated with PI3K-specific inhibitors, LY294002 or wortmannin, followed by treatment with insulin. Whereas FKHR level declined by insulin stimulation as presented above, PI3K inhibitors substantially inhibited the effect of insulin on FKHR degradation (Fig. 3*A*). Next, to examine the involvement of PI3K in FKHR ubiquitination signal, a dominant negative mutant of PI3K (Xp-Δp85) was cotransfected with FLAG-FKHR and HA-ubiquitin in HepG2 cells. Coexpression of Δp85 decreased FKHR ubiquitination accompanied with the reduced phosphorylation (Fig. 3*B*). These results suggest that insulin stimulation accelerates FKHR ubiquitination and degradation via a PI3K-signaling pathway. Moreover, to examine whether insulin-dependent ubiquitination of FKHR depends on the site-specific phosphorylation by PKB, an *in vivo* ubiquitination assay was performed by using FKHR phosphorylation site mutants. The individual T24A, S253A, and S316A mutants were ubiquitinated significantly lower than wild-type FKHR. Remarkably, the double mutants T24A/S253A, T24A/S316A, and S253A/S316A and the triple mutant (3A) were much less ubiquitinated than the one-point mutations (Fig. 3*C*). These results indicate that PKB-dependent phosphorylation plays a significant role for FKHR ubiquitination.

We further assessed the necessity of phosphorylation for FKHR ubiquitination by an *in vitro* ubiquitination assay using wild-type FLAG-FKHR or the 3A mutant that is immunoprecipitated from transfected HEK293T cell extracts. As illustrated in Fig. 3*D*, wild-type FKHR, but not the 3A mutant, was ubiquitinated in the presence of RRL, indicating that the phosphorylated state is required for FKHR ubiquitination.

Effect of Subcellular Localization on FKHR Ubiquitination. It has been shown that FOXO proteins are phosphorylated by insulin in the nucleus and exported to the cytoplasm (31, 32). Because we provide evidence that ubiquitination of FKHR requires its phosphorylation *in vivo* and *in vitro*, these observations contain several possibilities. First, phosphorylated FKHR is ubiquitinated in the nucleus and transported to the cytoplasm. Second, accumulation of phosphorylated FKHR in the cytoplasm promotes FKHR ubiquitination. Third, phosphorylated FKHR is ubiquitinated regardless of the subcellular localization. To distinguish these possibilities, we investigated the effect of the subcellular localization on FKHR ubiquitination by using the FKHR mutants (Fig. 4*A*): one was 3A/NLSm, in which both three PKB phosphorylation sites and arginine residues important for nuclear localization (31–33) were replaced by alanines; the other was NESm, in which the critical leucine and methionine residues in NES (8, 32) were converted to alanines. In the presence of serum, wild-type FKHR was localized in the cytoplasm, whereas 3A mutant was in the nucleus (Fig. 4 *B* and *C*). Remarkably, 3A/NLSm mutant was located in the cytoplasm, despite PKB-unphosphorylated form, in a major population of

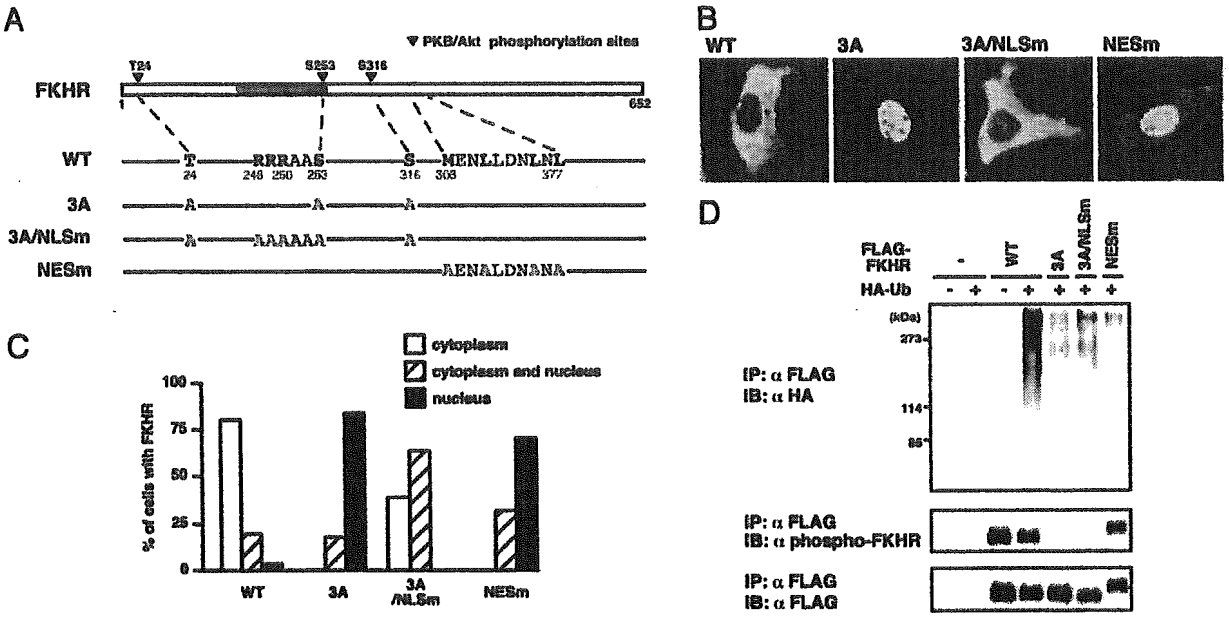

Fig. 4. Both phosphorylation and cytoplasmic retention are necessary for efficient FKHR ubiquitination. (*A*) A schematic representation of FKHR point mutants. The gray box indicates the forkhead DNA binding domain. (*B*) Localization of FKHR WT or mutants was monitored by transfection of these FKHRs into HepG2 cells in the presence of FBS and by immunolocalization with anti-FLAG antibody. (*C*) For quantitation, 100 cells per coverslips were counted, and the results are shown as the percentage of cells. (*D*) HepG2 cells were transfected with the indicated FKHR mutant and HA-ubiquitin expression plasmids and treated with MG132 in the presence of FBS. Whole cell extracts were subjected to anti-FLAG immunoprecipitation and followed by anti-HA (*Top*), anti-phospho-FKHR (*Middle*), or anti-FLAG (*Bottom*) immunoblotting.

transfected cells. In contrast, NESm mutant was predominantly localized in the nucleus, although this mutant was phosphorylated (Fig. 4 *B* and *C*, and *D Middle*). By using these mutants, we examined ubiquitination of FKHR *in vivo*. Both 3A/NLSm and NESm mutants, similar to 3A mutant, were much less ubiquitinated than wild-type (Fig. 4*D*). These results suggest that, in addition to the "phosphorylated" condition, the cytoplasmic retention is also necessary for efficient ubiquitination of FKHR.

Discussion

In this study, we have shown the degradation of FKHR phosphorylated by the PI3K-PKB pathway in response to insulin through the ubiquitin-proteasome system. Based on this finding, we speculate a mechanism for the regulation of FKHR by insulin (Fig. 5). When insulin binds to its specific receptor and activates the downstream signaling cascade, FKHR is phosphorylated by PKB and consequently excluded from the nucleus. Phosphorylated FKHR is then ubiquitinated in the cytoplasm, followed by degradation through the 26S proteasome. Recently, Plas and Thompson (34) have found that the expression of constitutively active PKB in hematopoietic cell line promotes proteasome-mediated decline of several PKB substrates, including FOXO1 (FKHR) and FOXO3 (FKHRL1). Our striking finding in the present study is that insulin triggers FKHR ubiquitination and proteasome-mediated degradation that require both phosphorylation and cytoplasmic retention.

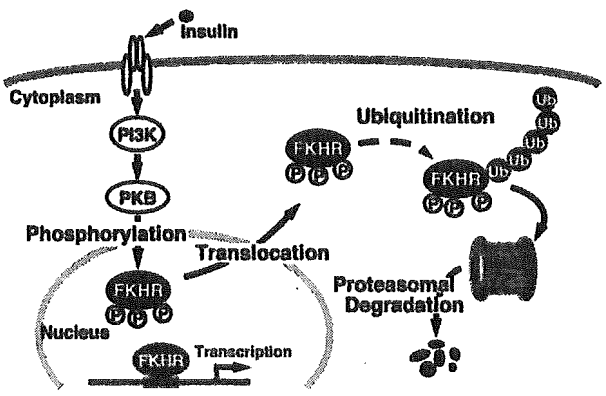

Fig. 5. A model for FKHR regulation through insulin-induced and phosphorylation-dependent degradation.

The ubiquitin-proteasome system is involved in the regulation of a variety of basic cellular processes. Ubiquitination is catalyzed through a multienzyme cascade, including the ubiquitin-activating enzyme (E1), the ubiquitin-conjugating enzyme (E2), and the ubiquitin ligase (E3) (30). The E3 enzymes accomplish the last and most essential step in the conjugation reaction with substrate specificity, and in several cases the target proteins are first marked by phosphorylation for ubiquitination. For example, IκB and β-catenin are phosphorylated by IκB-kinase complex and glycogen synthate kinase-3β, respectively, and then ubiquitinated by an Skp1/cullin-1/F-box protein: β-TrCP ($SCF^{\beta\text{-}TrCP}$), which selectively binds to phosphorylated serine residues of the substrates (35). In the case of FKHR, a strong correlation between phosphorylation and ubiquitination prompted us to consider the biochemical significance of phosphorylation as a prerequisite for ubiquitination. The first possibility is that an E3 enzyme may specifically require the phosphorylated residue(s) of FKHR to recognize and bind to it as a target. Second, the phosphorylation may induce conformational changes of FKHR, leading to exposure of the E3-binding domain, and thus permitting an E3 enzyme access to FKHR. Third, 14–3-3 proteins, which can associate with phosphorylated FOXO proteins (5, 32, 33), may affect the FKHR ubiquitination by mediating the interaction with an E3 enzyme.

Recent studies have demonstrated that subcellular localization also contributes to protein ubiquitination. Smad2 protein is phosphorylated and activated by transforming growth factor-β receptors and translocated to the nucleus, where it controls

transcription. Activated Smad2 is destroyed through the ubiquitin–proteasome pathway, in which its accumulation in the nucleus leads to ubiquitination mediated by Smurf2, whereas the receptor-phosphorylated region *per se* does not serve as a signal for ubiquitin conjugation (36–38). The p53 tumor suppressor protein levels are kept low during growth of normal cells through ubiquitination-mediated degradation, which is controlled by MDM2. p53 is ubiquitinated in the nucleus, exported to the cytoplasm, and degraded through proteasome (39). Our results indicate that insulin-induced export from the nucleus into the cytoplasm as well as phosphorylation is important for efficient FKHR ubiquitination, providing a novel mechanism of ubiquitination of proteins shuttling between the nucleus and the cytoplasm.

Given the physiological importance of insulin-dependent ubiquitination, the selective and irreversible degradation of phosphorylated FKHR subsequent to nuclear export may prevent the reentry of FKHR into the nucleus and principally contribute to sustaining the inhibitory effect of insulin on gene expression. Therefore, further studies to identify the E3 enzyme for FKHR would be expected to provide new insights into the mechanism by which insulin regulates FKHR function and gene expression.

We especially thank Dr. Wataru Ogawa, Kobe University, for the gift of the plasmid (pGEX-Δp85). We also thank the Fukamizu laboratory members for their helpful discussion and encouragement. This work was supported by The 21st Century COE Program, Grant-in-Aid for Scientific Research (A), and Grant-in-Aid for Scientific Research on Priority Areas from the Ministry of Education, Science, Sports, and Technology of Japan, "Research for the Future" Program (The Japan Society for the Promotion of Science JSPS-RFTF 97L00804), the Research Grant for Cardiovascular Diseases (11C-1), Comprehensive Research on Aging and Health from the Ministry of Health, Labour, and Welfare, TAKEDA Science Foundation, and The Cell Science Research Foundation.

1. Kandel, E. S. & Hay, N. (1999) *Exp. Cell Res.* **253,** 210–229.
2. Kido, Y., Nakae, J. & Accili, D. (2001) *J. Clin. Endocrinol. Metab.* **86,** 972–979.
3. Burgering, B. M. & Kops, G. J. (2002) *Trends Biochem. Sci.* **27,** 352–360.
4. Birkenkamp, K. U. & Coffer, P. J. (2003) *Biochem. Soc. Trans.* **31,** 292–297.
5. Brunet, A., Bonni, A., Zigmond, M. J., Lin, M. Z., Juo, P., Hu, L. S., Anderson, M. J., Arden, K. C., Blenis, J. & Greenberg, M. E. (1999) *Cell* **96,** 857–868.
6. Kops, G. J., de Ruiter, N. D., De Vries-Smits, A. M., Powell, D. R., Bos, J. L. & Burgering, B. M. (1999) *Nature* **398,** 630–634.
7. Rena, G., Guo, S., Cichy, S. C., Unterman, T. G. & Cohen, P. (1999) *J. Biol. Chem.* **274,** 17179–17183.
8. Biggs, W. H., III, Meisenhelder, J., Hunter, T., Cavenee, W. K. & Arden, K. C. (1999) *Proc. Natl. Acad. Sci. USA* **96,** 7421–7426.
9. Takaishi, H., Konishi, H., Matsuzaki, H., Ono, Y., Shirai, Y., Saito, N., Kitamura, T., Ogawa, W., Kasuga, M., Kikkawa, U. & Nishizuka, Y. (1999) *Proc. Natl. Acad. Sci. USA* **96,** 11836–11841.
10. Ayala, J. E., Streeper, R. S., Desgrosellier, J. S., Durham, S. K., Suwanichkul, A., Svitek, C. A., Goldman, J. K., Barr, F. G., Powell, D. R. & O'Brien, R. M. (1999) *Diabetes* **48,** 1885–1889.
11. Schmoll, D., Walker, K. S., Alessi, D. R., Grempler, R., Burchell, A., Guo, S., Walther, R. & Unterman, T. G. (2000) *J. Biol. Chem.* **275,** 36324–36333.
12. Hall, R. K., Yamasaki, T., Kucera, T., Waltner-Law, M., O'Brien, R. & Granner, D. K. (2000) *J. Biol. Chem.* **275,** 30169–30175.
13. Daitoku, H., Yamagata, K., Matsuzaki, H., Hatta, M. & Fukamizu, A. (2003) *Diabetes* **52,** 642–649.
14. Nakae, J., Biggs, W. H., III, Kitamura, T., Cavenee, W. K., Wright, C. V., Arden, K. C. & Accili, D. (2002) *Nat. Genet.* **32,** 245–253.
15. Taub, J., Lau, J. F., Ma, C., Hahn, J. H., Hoque, R., Rothblatt, J. & Chalfie, M. (1999) *Nature* **399,** 162–166.
16. Honda, Y. & Honda, S. (1999) *FASEB J.* **13,** 1385–1393.
17. Ishii, N., Goto, S. & Hartman, P. S. (2002) *Free Radical Biol. Med.* **33,** 1021–1025.
18. Nemoto, S. & Finkel, T. (2002) *Science* **295,** 2450–2452.
19. Kops, G. J., Dansen, T. B., Polderman, P. E., Saarloos, I., Wirtz, K. W., Coffer, P. J., Huang, T. T., Bos, J. L., Medema, R. H. & Burgering, B. M. (2002) *Nature* **419,** 316–321.
20. Zhao, H. H., Herrera, R. E., Coronado-Heinsohn, E., Yang, M. C., Ludes-Meyers, J. H., Seybold-Tilson, K. J., Nawaz, Z., Yee, D., Barr, F. G., Diab, S. G., *et al.* (2001) *J. Biol. Chem.* **276,** 27907–27912.
21. Schuur, E. R., Loktev, A. V., Sharma, M., Sun, Z., Roth, R. A. & Weigel, R. J. (2001) *J. Biol. Chem.* **276,** 33554–33560.
22. Hirota, K., Daitoku, H., Matsuzaki, H., Araya, N., Yamagata, K., Asada, S., Sugaya, T. & Fukamizu, A. (2003) *J. Biol. Chem.* **278,** 13056–13060.
23. Hatta, M., Daitoku, H., Matsuzaki, H., Deyama, Y., Yoshimura, Y., Suzuki, K., Matsumoto, A. & Fukamizu, A. (2002) *Int. J. Mol. Med.* **9,** 147–152.
24. Ebisawa, T., Fukuchi, M., Murakami, G., Chiba, T., Tanaka, K., Imamura, T. & Miyazono, K. (2001) *J. Biol. Chem.* **276,** 12477–12480.
25. Kotani, K., Yonezawa, K., Hara, K., Ueda, H., Kitamura, Y., Sakaue, H., Ando, A., Chavanieu, A., Calas, B., Grigorescu, F., *et al.* (1994) *EMBO J.* **13,** 2313–2321.
26. de Hoog, C. L., Koehler, J. A., Goldstein, M. D., Taylor, P., Figeys, D. & Moran, M. F. (2001) *Mol. Cell. Biol.* **21,** 2107–2117.
27. Pagano, M., Tam, S. W., Theodoras, A. M., Beer-Romero, P., Del Sal, G., Chau, V., Yew, P. R., Draetta, G. F. & Rolfe, M. (1995) *Science* **269,** 682–685.
28. Conaway, R. C., Brower, C. S. & Conaway, J. W. (2002) *Science* **296,** 1254–1258.
29. Desterro, J. M., Rodriguez, M. S. & Hay, R. T. (2000) *Cell. Mol. Life Sci.* **57,** 1207–1219.
30. Weissman, A. M. (2001) *Nat. Rev. Mol. Cell. Biol.* **2,** 169–178.
31. Brownawell, A. M., Kops, G. J., Macara, I. G. & Burgering, B. M. (2001) *Mol. Cell. Biol.* **21,** 3534–3546.
32. Brunet, A., Kanai, F., Stehn, J., Xu, J., Sarbassova, D., Frangioni, J. V., Dalal, S. N., DeCaprio, J. A., Greenberg, M. E. & Yaffe, M. B. (2002) *J. Cell. Biol.* **156,** 817–828.
33. Rena, G., Prescott, A. R., Guo, S., Cohen, P. & Unterman, T. G. (2001) *Biochem. J.* **354,** 605–612.
34. Plas, D. R. & Thompson, C. B. (2003) *J. Biol. Chem.* **278,** 12361–12366.
35. Maniatis, T. (1999) *Genes Dev.* **13,** 505–510.
36. Lo, R. S. & Massague, J. (1999) *Nat. Cell Biol.* **1,** 472–478.
37. Lin, X., Liang, M. & Feng, X. H. (2000) *J. Biol. Chem.* **275,** 36818–36822.
38. Zhang, Y., Chang, C., Gehling, D. J., Hemmati-Brivanlou, A. & Derynck, R. (2001) *Proc. Natl. Acad. Sci. USA* **98,** 974–979.
39. Michael, D. & Oren, M. (2003) *Semin. Cancer Biol.* **13,** 49–58.

THE JOURNAL OF BIOLOGICAL CHEMISTRY
Vol. 278, No. 43, Issue of October 24, pp. 41890–41899, 2003
Printed in U.S.A.

Parkin Cleaves Intracellular α-Synuclein Inclusions via the Activation of Calpain*

Received for publication, June 9, 2003, and in revised form, August 5, 2003
Published, JBC Papers in Press, August 12, 2003, DOI 10.1074/jbc.M306017200

Se Jung Kim‡§, Jee Young Sung‡§, Ji Won Um¶, Nobutaka Hattori‖, Yoshikuni Mizuno‖, Keiji Tanaka, Seung R. Paik‡‡, Jongsun Kim§ §§, and Kwang Chul Chung¶ ¶¶**

*From the ¶Department of Biology, Yonsei University College of Sciences, ‡Department of Medical Science, §§Department of Microbiology, and §Brain Korea 21 Projects for Medical Science, Yonsei University College of Medicine, Shinchon-dong 134, Seodaemun-gu, Seoul 120-749, Korea, the ‡‡Department of Biochemistry, College of Medicine, Inha University, Inchon 402-751, Korea, the ‖Department of Neurology, Juntendo University School of Medicine, Tokyo 113-8421, Japan, and **Tokyo Metropolitan Institute of Medical Science, Tokyo 113-8613, Japan*

Mutations in the α-synuclein and parkin genes cause heritable forms of Parkinson's disease. In the present study, we examined the possible functional relationship between the parkin and α-synuclein genes in a conditionally immortalized embryonic hippocampal cell (H19-7) line. Whereas transient transfection of α-synuclein into neuronal H19-7 cells caused the formation of its intracytoplasmic inclusions and a significant cell death, the combined overexpression of parkin restored the α-synuclein-induced decrease in cell viability to control levels. In addition, the overexpression of parkin was found to generate selective cleavage of α-synuclein. Furthermore, the cytoprotective effect of parkin on α-synuclein-induced cell death was not inhibited in the presence of a proteasome inhibitor. Interestingly, the overexpression of parkin induced the activation of an intracellular cysteine protease, calpain, but not caspase, and the cytoprotective effect of parkin on α-synuclein cytotoxicity was significantly inhibited by the presence of calpain-specific inhibitors. In conclusion, our results suggest that parkin accelerates the degradation of α-synuclein via the activation of the nonproteasomal protease, calpain, leading to the prevention of α-synuclein-induced cell death in embryonic hippocampal progenitor cells.

Parkinson's disease (PD)[1] is a common neurodegenerative disorder involving the deterioration of dopaminergic neurons in the pars compacta region of the substantia nigra (1). PD patients suffer from rigidity, slowness of movement, tremor, and lack of balance. The etiology of PD is poorly understood, but genetic factors are believed to play an important role in its pathophysiology (2, 3). It has been reported that familial PD involves mutations in three different genes. First, two missense mutations of the α-synuclein gene have been linked to familial PD (4). α-Synuclein is a major component of Lewy bodies (LBs), the pathological hallmark of PD and dementia with LBs (5). Second, the ubiquitin carboxyl-terminal hydrolase-L1 (UCH-L1) gene has also been linked to some cases of familial PD. A missense mutation in UCH-L1 was identified in two members of the same kin having early onset autosomal dominant and typical PD (6). UCH-L1 appears to be involved in scavenging the ubiquitin peptide after the ubiquitin molecule has tagged the damaged molecules for proteasomal degradation. Third, parkin is the causative gene of early onset autosomal recessive juvenile Parkinsonism (AR-JP) (7, 8). Recently, parkin has been reported to be an ubiquitin-protein ligase E3 (9, 10). Various mutations of parkin have been reported in AR-JP patients, including exon deletion, exon multiplication and point mutation (11). Parkin consists of two functionally different domains: the C-terminal RING box, which recruits a specific E2 enzyme, and the N-terminal ubiquitin-like (Ubl) domain required for the recognition of the target protein, which is to be ubiquitinated before proteasomal degradation. Various mutations of parkin are believed to be involved in the impairment of the normal metabolism of target proteins by proteasome, and the accumulations of unknown protein may cause AR-JP.

Whereas missense mutations in α-synuclein or UCH-L1 cause rare autosomal dominant forms of PD, mutations of parkin are a relatively common cause of AR-JP. As is the case in conventional idiopathic PD, the neuropathologic changes of parkin-linked AR-JP are largely confined to the brain stem and include the loss of selected neurons and local gliosis. However, α-synuclein- and ubiquitin-positive neuronal inclusions, LBs, are generally absent in parkin-linked AR-JP (11–13).

Based on the mutation in UCH-L1 and parkin, it is suggested that the impaired proteasomal degradation of abnormal proteins seems to underlie the pathogenesis of PD. In addition, the previous report that the mRNA expression patterns of parkin and α-synuclein are remarkably similar (14) suggested that these two proteins may be involved in common pathways, which contribute to the pathophysiology of PD. The substrate proteins for parkin remain largely unknown, with the exception of CDCrel-1 (15) and the Pael receptor (16). In PD, parkin is co-localized in some LBs (17) and all axonal spheroids (18), which contain aggregated α-synuclein. The association be-

* This work was supported by the Neurobiology Research Program from the Korea Ministry of Science and Technology (to K. C. C), partly by the Basic Research program of Korea Science and Engineering Foundation (to K. C. C.), by the Korea Health 21 R&D Project, Ministry of Health & Welfare (03-PJ1-PG10-21300-0023) (to K. C. C.), and by the Brain Korea 21 Projects for Medical Science in Yonsei University (to S. J. K and J. Y. S.). The costs of publication of this article were defrayed in part by the payment of page charges. This article must therefore be hereby marked "*advertisement*" in accordance with 18 U.S.C. Section 1734 solely to indicate this fact.

¶¶ To whom correspondence should be addressed. Tel.: 82-2-2123-2653; Fax: 82-2-312-5657; E-mail: kchung@yonsei.ac.kr.

[1] The abbreviations used are: PD, Parkinson's disease; Ac-DEVD-*p*NA, acetyl-Asp-Glu-Val-Asp-*p*-nitroaniline; AR-JP, autosomal recessive juvenile Parkinsonism; DMEM, Dulbecco's modified Eagle medium; GFP, green fluorescent protein; LB, Lewy body; MTT, 3-(4,5-dimethylthiazol-2-yl)-2,5-diphenyltetrazolium bromide; PARP, poly(ADP-ribose) polymerase; Suc, *N*-succinyl; Suc-LLVY-AMC, Suc-Leu-Leu-Val-Tyr-7-amino-4-methylcoumarin; AMC, 7-amino-4-methylcoumarin; Ub, ubiquitin; Ubl, ub-like; UCH-L1, ubiquitin carboxyl-terminal hydrolase L1; E1, ubiquitin-activating enzyme; E2, ubiquitin carrier protein; E3, ubiquitin-protein isopeptide ligase; PBS, phosphate-buffered saline; CMAC, 7-amino-4-chloromethylcoumarin; *Z*-VAD-fmk, *N*-benzyloxycarbonyl-Val-Ala-Asp fluoromethyl ketone.

tween parkin and α-synuclein in LB suggests that parkin interacts with α-synuclein, and this interaction may play a role in the pathogenesis of PD. On the basis of the above reports, the objective of the present study was to investigate the functional relationship between parkin and α-synuclein in immortalized hippocampal progenitor cells.

EXPERIMENTAL PROCEDURES

Materials—Fetal bovine serum, Dulbecco's modified Eagle's medium (DMEM), and Geneticin were purchased from Invitrogen. Plasmids encoding epitope-tagged human wild type parkin (pcDNA3.1Myc-parkin) and its serial deletion mutants, amino acids 77–465, 217–465, 295–465, 1–415, and 1–310 of parkin, cloned in pcDNA3.1-Myc vectors were prepared, as described elsewhere (9). Plasmid, used to express jellyfish green fluorescent protein, fused with a noncleavable mutant ubiquitin (Ub) moiety as a substrate for ubiquitin-proteasome-dependent proteolysis, $Ub^{G76V}GFP$, was a gift from M. Masucci (Karolinska Institute, Stockholm, Sweden). Clastolactacystin β-lactone and *N*-succinyl-Leu-Leu-Val-Tyr-7-amino-4-methylcoumarin (Suc-LLVY-AMC) were purchased from Biomol; a colorimetric caspase substrate, acetyl-DEVD-*p*-nitroaniline, calpastatin peptide, and calpeptin were from Calbiochem; and monoclonal antibody against β-*O*-linked *N*-acetylglucosamine was purchased from Babco. Rhodamine-conjugated secondary antibodies were purchased from Sigma, and polyclonal anti-Myc and anti-PARP antibodies were purchased from Santa Cruz Biotechnology, Inc. (Santa Cruz, CA). All other chemicals used were commercial products of analytical grade obtained from Sigma.

Cell Culture and DNA Transfection—The rat neuronal hippocampal progenitor cell line (H19-7) was generated by transduction with retroviral vectors containing a temperature-sensitive SV40 large T antigen, which is functionally active at 33 °C and inactive at 39 °C (19). The undifferentiated and proliferating H19-7 cells were grown in DMEM containing 10% fetal bovine serum at 33 °C and maintained under the selection of 200 g/ml G418. The cells were transfected with various expression vectors using LipofectAMINE plus reagent (Invitrogen), according to the manufacturer's instructions. The total amount of DNA in each individual transfection experiment was adjusted by using parental empty vector DNA. The cells were cultured for at least 24 h after transfection and used in the subsequent immunoprecipitation, Western blot analysis, and cell viability assay experiments.

Assessment of Cell Viability by 3-(4,5-Dimethylthiazol-2-yl)-2,5-diphenyltetrazolium Bromide (MTT) Extraction Assay—Quantitation of cell survival was performed using the tetrazolium salt extraction method (20). 62.5 μl of the 5 mg/ml stock solution of MTT was added to each well containing 250 μl of medium in a 24-well plate. After a 2-h incubation at 37 °C, 250 μl of extraction buffer containing 20% SDS and 50% *N*,*N*-dimethylformamide, at pH 7.4, was added. After incubating the reagents overnight at 37 °C, the optical density was measured at 570 nm using a SpectraMAX340 enzyme-linked immunosorbent assay reader (Molecular Devices, Sunnyvale, CA), with extraction buffer used as a standard. Statistical analyses were completed with the aid of the StatView II program for Macintosh computers (Abacus Concepts). All data were analyzed by one-way analysis of variance, and preplanned comparisons with the control were performed by Dunnett's T-statistic.

Immunoprecipitation and Western Blot Analysis—The H19-7 cells were transfected with a mammalian expression vector using LipofectAMINE. Forty-eight hours later, the cells were washed with cold PBS buffer and harvested in lysis buffer containing 1% Triton X-100, 1 μg/ml aprotinin, 1 μg/ml leupeptin, 200 μM phenylmethylsulfonyl fluoride, 1 mM Na_3VO_4, and 10 mM NaF. The supernatant was then preincubated at 4 °C overnight with anti-Myc antibody (Santa Cruz Biotechnology, Inc., Santa Cruz, CA). The supernatant was combined with 30 μl of Protein A-Sepharose (Amersham Biosciences) and left at 4 °C for 2 h, followed by being washed thoroughly three times with lysis buffer. The precipitate was resolved on SDS-PAGE gel and subjected to Western blot analysis.

Pulse-chasing Analysis of α-Synuclein—After H19-7 cells were transiently transfected with the plasmids encoding α-synuclein or/and parkin in H19-7 cells for 24 h, the cells were washed in PBS and incubated with methionine-free DMEM and labeled with [^{35}S]methionine (10 μCi/ml) for 8 h and washed in PBS. Next the cells were washed extensively with DMEM, incubated with DMEM, and lysed in TLB. Primary antibody against α-synuclein was added to the cell lysates, and the Protein A-Sepharose bead samples were added to cell lysate mixtures and incubated for 1 h. Immunoprecipitated samples were washed three times in lysis buffer and solubilized by boiling the sample for 5 min. After electrophoresis, the gel was stained with Coomassie Blue dye, dried, and analyzed by autoradiography.

Measurement of Calpain and Caspase-3 Activity Using a Fluorescent Substrate Peptide—The activities of calpain and caspase-3 can be determined using the highly fluorescent peptide substrate, Suc-LLVY-AMC, for calpain and a colorimetric acetyl-Asp-Glu-Val-Asp-*p*-nitroaniline (Ac-DEVD-*p*NA) for caspase. After either Suc-LLVY-AMC (80 μM) or Ac-DEVD-*p*NA (10 μM) was added to the cells, the cell culture medium was harvested for assay of cleaved AMC and *p*NA. The formation of AMC was detected at $\lambda_{EX} = 380/\lambda_{EM} = 460$ by spectrofluorometer (PerkinElmer Life Sciences), whereas cleavage of *p*NA was monitored colorimetrically at 405 nm by spectrophotometer (Bio-Rad). To measure the *in situ* calpain activity in individual neuronal cells using Boc-Leu-Met-7-amino-4-chloromethylcoumarin (Boc-Leu-Met-CMAC), the H19-7 cells were mounted on fluorescence microscopy (excitation 380 nm; a dichronic cut-off of 430 nm with emission wavelength of 510 nm). Then cell-permeable calpain substrate, Boc-Leu-Met conjugated to the fluorophore CMAC (Boc-Leu-Met-CMAC, Molecular Probes, Inc., Eugene, OR) in Me_2SO, was added to the cells at a final concentration of 20 μM. Whereas the change in fluorescence over time intervals of 30–60 s was measured to minimize photobleaching, the average calpain activity in the cells to express Myc-parkin (minimum of five cells) was measured. Where specified, either calpain inhibitor or ionomycin was added to the cells, and the calpain activity was assessed in each individual cell.

Indirect Fluorescence Microscopy—To assess the individual cells to overexpress parkin, H19-7 cells grown in 6-well plates on coverslips were transiently transfected with the Myc-parkin construct. Cells were then incubated with primary anti-Myc antibody for 1 h at 4 °C in DMEM supplemented with 1% bovine serum albumin and washed twice with PBS. The cells were then fixed with 3.7% formaldehyde/PBS for 15 min, washed with PBS, and permeabilized with 0.05% Triton X-100/PBS for 10 min at room temperature. Nonspecific binding was blocked with blocking solution (0.05% Triton X-100/PBS containing 5% nonfat dry milk) for 30 min at 37 °C. Goat anti-mouse rhodamine-conjugated secondary antibody was then added for 1 h at 37 °C. The cells were then washed seven times with 0.05% Triton X-100/PBS. Finally, the cells were fixed again with 3.7% formaldehyde. Coverslips were observed under Olympus epifluorescence microscope equipped with a fluorescence filter. Digital images of cells were recorded using a Leica DC200 camera.

RESULTS

Parkin Selectively Binds to α-Synuclein in Hippocampal Progenitor H19-7 Cells—The parkin gene has been reported to be expressed in various stages of the central nervous system developmental process (21). In both the rat and the mouse, parkin begins to be expressed at embryonic 15 days, and this continues until the late stage of fetal life in a manner parallel to that of central nervous system neural development. First, we examined whether parkin was expressed in our model system, a conditionally immortalized embryonic hippocampal progenitor cell line (H19-7). After the cell lysates were prepared from undifferentiated and proliferating H19-7 cells, the presence of the parkin protein was determined by Western blot analysis using polyclonal anti-parkin antibodies. As shown in Fig. 1*A*, the expression of parkin, corresponding to a molecular size of 52 kDa, was identified with an additional, unknown 50-kDa band, indicating that parkin is endogenously and significantly expressed in H19-7 cells. To detect the epitope-tagging parkin protein after the transient transfection of its construct into H19-7 cells, Western blot analysis was performed with anti-Myc antibodies. Compared with the mock-transfected control cells, the expression of the recombinant fusion proteins of parkin with the Myc peptide was identified (Fig. 1*A*). However, we had previously observed that the endogenous protein level of α-synuclein is too low to be detected in H19-7 cells (22).

Second, in order to clarify the relationship between parkin and α-synuclein, we checked whether parkin binds to α-synuclein in a specific way in H19-7 cells. In a previous study, we observed that the exogenous addition of bacterially recombinant α-synuclein proteins leads to their intracellular transport, subsequently causing a significant necrotic-like cell

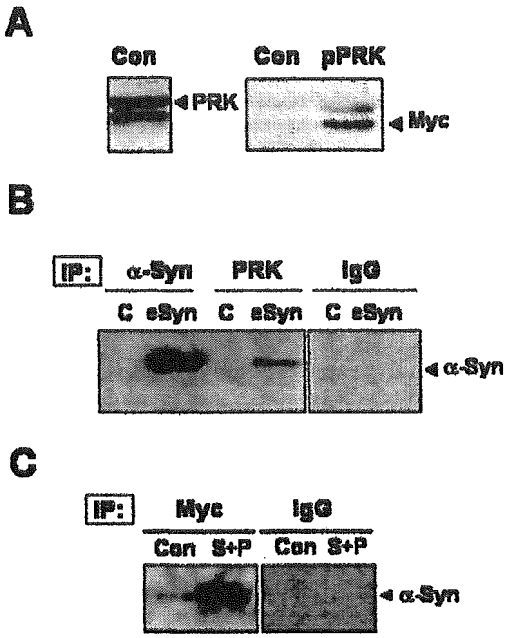

FIG. 1. **Parkin interacts with α-synuclein in embryonic hippocampal progenitor H19-7 cells.** *A*, where specified, H19-7 cells were mock-transfected (*Con*) or transfected with 5 μg of eukaryotic expression vector DNA to encode Myc-tagged wild type parkin protein (*pPRK*) in a transient manner. After 48 h of incubation, the cell lysates were prepared, and the presence of parkin (*PRK*) was determined by using Western blot analysis with anti-parkin or anti-Myc antibodies (*Myc*), as indicated. *B* and *C*, H19-7 cells were either untreated (*C*) or treated with bacterially expressed α-synuclein proteins (10 μM; *eSyn*) for 1 h (*B*), as indicated. Where specified, the cells were transiently co-transfected with 5 μg of each plasmid encoding Myc-tagged parkin plus α-synuclein (*P + S*), respectively, for 48 h. After incubation, immunoprecipitation (*IP*) was performed with anti-Parkin, anti-Myc antibodies, or mouse control IgGs, as indicated. Then, the immunocomplexes were resolved by SDS-PAGE and analyzed by Western blot analysis with monoclonal anti-α-synuclein antibodies (*α-Syn*).

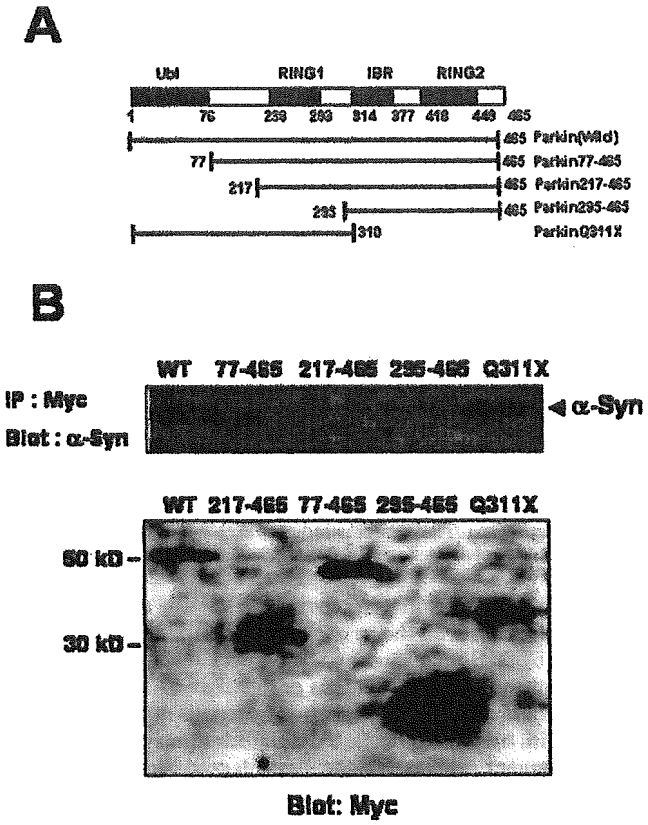

FIG. 2. **Domain analysis of parkin interacting with α-synuclein.** *A*, diagram depicting wild type (*WT*) and various deletion mutants of parkin protein. *B*, analysis of molecular interaction between wild type α-synuclein and several deletion mutants of parkin. Where indicated, 5 μg of plasmid encoding Myc-tagged whole parkin protein or its deleted mutant, respectively, was co-transfected with an eukaryotic expression vector (5 μg) to express wild type α-synuclein into H19-7 cells. Immunoprecipitaion (*IP*) was performed with anti-Myc antibodies, and immunoprecipitates were analyzed by Western blot analysis with either anti-α-synuclein (α-Syn) or anti-Myc antibodies.

death in the H19-7 cell (22). The neuronal cell death appeared to be correlated with the Rab5A-specific endocytosis of α-synuclein that subsequently caused the formation of Lewy body-like intracytoplasmic inclusions. This was further supported by the fact that the expression of GTPase-deficient Rab5A resulted in a significant decrease of its cytotoxicity as a result of incomplete endocytosis of α-synuclein (22). To determine whether exogenous α-synuclein interacts with parkin, 10 μM α-synuclein was added to the cells for 1 h, and then immunoprecipitation was performed using the anti-parkin antibody. Western blot analysis with anti-α-synuclein antibodies showed evidence of the expression of α-synuclein with an approximate 19-kDa molecular size in the immunoprecipitated protein complexes, indicating that intracellular parkin binds to α-synuclein (Fig. 1*B*). In order to determine whether intracellular transfected α-synuclein also binds to parkin, two mammalian expression vectors encoding α-synuclein and Myc-tagged parkin (pcDNA3.1-Myc/His), respectively, were co-transfected into the H19-7 cells in a transient manner. After 48 h, immunoprecipitation was performed with an anti-Myc antibody, and the precipitates were analyzed by Western blot analysis using the anti-α-synuclein antibody. As shown in Fig. 1*C*, parkin selectively binds to α-synuclein. These findings suggest that parkin is functionally linked to α-synuclein in the embryonic hippocampal cell lines.

Parkin Binds to α-Synuclein through Its Ubl Domain—To explore the domain in parkin that is associated with its interaction with α-synuclein, binding assays were performed using several deletion mutants of parkin (Fig. 2*A*). Plasmids, encoding a series of deletion parkin mutants with Myc tag, were co-transfected into H19-7 cells using a plasmid to express wild type α-synuclein, followed by immunoprecipitation with anti-α-synuclein IgG. Apart from the whole complete protein, only the peptide, with its N-terminal portion of parkin remaining intact, still retained the binding activity to α-synuclein, whereas the peptide with its C-terminal part intact did not retain this binding activity (Fig. 2*B*). Moreover, the loss of the N-terminal Ubl domain of parkin resulted in the complete failure of the specific interaction with α-synuclein, indicating that the Ubl domain of parkin is essential for its binding to α-synuclein.

Parkin Suppresses the α-Synuclein-induced Cytotoxicity via the Selective Degradation of Its Intracytoplasmic Inclusions—Next, to examine the physiological relevance of the specific binding between α-synuclein and parkin, the effect of intracellular overexpression of α-synuclein on cell viability was assessed. Following the transient transfection of a plasmid encoding α-synuclein into H19-7 cells, the change of cell viability was measured after 24 h by means of the MTT extraction method. As shown in Fig. 3, the overexpression of α-synuclein decreased cell viability in H19-7 cells. Interestingly, when α-synuclein was co-expressed with parkin, simultaneously, parkin significantly suppressed α-synuclein-induced cell death (Fig. 3). Meanwhile, the overexpression of parkin alone has no remarkable effect on cell viability. These data indicated that the overexpression of α-synuclein leads to neuronal cell

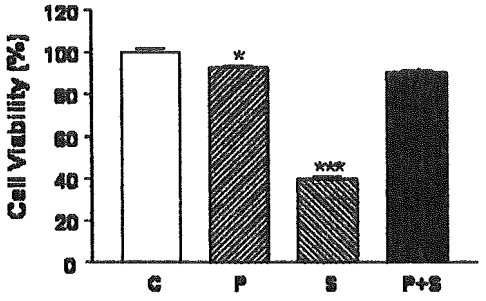

FIG. 3. **Overexpression of Parkin selectively suppresses α-synuclein-induced cell death in H19-7 cells.** Where specified, H19-7 cells were transiently transfected with a construct (5 μg) encoding parkin (*P*), or α-synuclein (*S*), respectively. Otherwise, the cells were co-transfected with a parkin plasmid (5 μg) plus cDNA construct encoding α-synuclein (5 μg) (*P* + *S*). Prior to assessing cell viability, the cells were shifted to an environment of neuronal differentiation with the temperature of 39 °C under an N_2 medium. After incubation for 48 h, cell viability was determined by MTT extraction assay. Data are expressed as mean ± S.E. from three-independent experiments conducted in triplicate. The *asterisks* indicate significant differences compared with control cells. *, $p < 0.05$; ***, $p < 0.001$.

death, whereas parkin selectively blocks the cytotoxicity of α-synuclein. Based on the previous findings that α-synuclein is degraded by 26 S proteasome (22) and parkin acts as ubiquitin-protein ligase E3 (9, 10, 23), the protective effect of parkin on α-synuclein toxicity could be exerted by means of the removal of α-synuclein, by parkin-mediated ubiquitination of α-synuclein and subsequent proteasome-mediated degradation. Previously, we have shown that the H19-7 cells were not found to contain any significant levels of α-synuclein (22), which is consistent with a previous report in which α-synuclein only begins to be expressed after the post-natal period in the rat central nervous system (24). To ascertain whether parkin controls the degradation of intracellular α-synuclein, H19-7 cells were transiently transfected with either a plasmid encoding α-synuclein or parkin. Western blot analysis with anti-Myc or anti-α-synuclein antibodies confirmed that α-synuclein and parkin were properly expressed inside the cells (Fig. 4*A*). However, when the plasmids of both α-synuclein and parkin were co-transfected into H19-7 cells, the levels of intracellular α-synuclein were significantly diminished in proportion to the amount of parkin DNA to be transfected (Fig. 4*B*). In addition to the measurement of steady state levels of α-synuclein, a pulse-chase experiment was performed to determine the rate of α-synuclein degradation. After H19-7 cells were transfected with either an expression vector encoding α-synuclein alone or with parkin plasmid in a transient manner, both cells were metabolically labeled with [^{35}S]methionine, and the cell lysates were immunoprecipitated with anti-α-synuclein antibodies. As shown in Fig. 4*C*, co-transfection of parkin plus α-synuclein led to a significant increase in the rate of α-synuclein degradation in a dose-dependent way of the amount of parkin-encoding construct, compared with control cells transfected with α-synuclein alone (Fig. 4*C*). These findings suggested that parkin promotes the degradation of α-synuclein in H19-7 cells. In addition, the cytoprotective effect of parkin on α-synuclein-induced neurotoxicity was found to be proportional to the amount of parkin plasmids to be transfected (data not shown).

Based on the recent report by Shimura *et al.* that parkin binds and ubiquitinates the 22-kDa glycosylated form of α-synuclein as its substrate, but not its intact form in normal human brain (13), we next examined whether the transiently expressed α-synuclein had been glycosylated via the post-translational modification within its serine or/and threonine residues. β-*O*-Linked *N*-acetylglucosamine (*O*-GlcNAc) is an abundant post-translational modification occurring on serine and threonine residues. This modification has been detected on a variety of nuclear and cytoplasmic proteins involved in diverse cellular functions (25). To determine whether parkin interacts with *O*-linked glycosylated α-synuclein in H19-7 cells, co-immunoprecipitation experiments were performed by using α-synuclein antibodies for immunoprecipitation, followed by immunoblotting with either α-synuclein antibody or well characterized monoclonal antibodies for Ser-*O*-GlcNAc and Thr-*O*-GlcNAc residues. Whereas the 18-kDa α-synuclein protein was specifically precipitated by its antibody in all cases, *O*-glycosylated GlcNAc antibodies failed to detect the α-synuclein (Fig. 4*D*). Since the specific DNA binding activity of transcription factor p53 is known to be regulated by the *O*-glycosylation at its carboxyl-terminal charged residues (43, 48), the modification of p53 protein by *O*-GlcNAc, which was identified by the immunoprecipitation against p53 antibodies followed by immunoblotting with anti-*O*-GlcNAc IgG, was used as a positive control for anti-*O*-GlcNAc antiserum in H19-7 cells (Fig. 4*D*). These immunochemical results suggest that nonglycosylated α-synuclein binds to parkin and that the protective effect of parkin on α-synuclein-induced cytotoxicity has its origin in the parkin-induced degradation of α-synuclein in H19-7 cells.

Immunocytochemical visualization of the cells clearly showed that the distribution of transiently transfected α-synuclein is uneven and took the form of granular aggregates in the cytoplasm (Fig. 4*E*). Previously, we have shown that the addition of recombinant α-synuclein to H19-7 cells leads to neuronal cell death, which appears to be closely associated with the formation of intracytoplasmic α-synuclein inclusions. In addition, the components of these α-synuclein-positive inclusions were very similar to those of Lewy body inclusions in PD patients (22). However, the co-transfection of parkin plus α-synuclein resulted in the degradation of α-synuclein-positive inclusions, suggesting that the intracellular formation of granular α-synuclein's accumulation correlates well with its neurotoxicity in H19-7 cells.

Parkin-mediated Degradation of α-Synuclein Occurs via a Proteasome-independent Pathway—To test the possibility that parkin-induced degradation of α-synuclein includes the activation of the ubiquitin-proteasome pathway, the effect of parkin on α-synuclein-induced cytotoxicity was tested, under the blockade of proteasomal proteolysis, by using its highly specific inhibitor, clastolactacystin β-lactone. First, when H19-7 cells were stimulated with this drug alone, no significant change in cell viability was produced (Fig. 5). Likewise, the overexpression of parkin alone did not affect cell viability, irrespective of the absence or presence of proteasomal inhibitor. Transient transfection of the cells with α-synuclein followed by stimulation with clastolactacystin β-lactone significantly decreased cell viability, compared with that in cells transfected with α-synuclein alone (Fig. 5). Based on the previous report that α-synuclein is degraded by the ubiquitin-proteasome system, our finding also strongly indicated that α-synuclein could be degraded via the ubiquitin-proteasomal proteolytic pathway in neuronal H19-7 cells. The more toxic effect of α-synuclein in the presence of proteasomal inhibitor was thought to arise from the suppression of the proteasomal proteolytic machinery. However, when the plasmids encoding parkin and synuclein were co-transfected into H19-7 cells, the expected decrease in cell viability, caused by parkin, was not prevented in the presence of clastolactacystin β-lactone (Fig. 5). These data suggested that the cytoprotective effect of parkin on α-synuclein may be mediated by the activation of some other proteasome-independent proteolytic machinery.

In addition, the effect of parkin on the ubiquitin-proteasome-dependent proteolytic pathways was assessed by using the

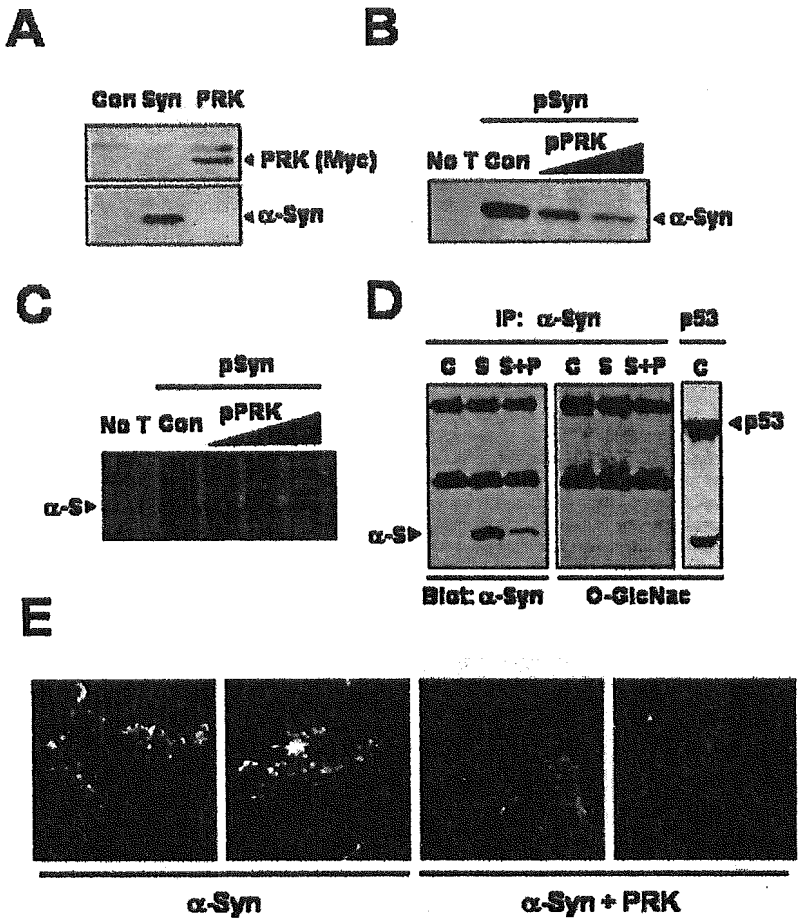

FIG. 4. **Parkin enhances the degradation of nonglycosylated α-synuclein in H19-7 cells.** *A*, where specified, H19-7 cells were mock-transfected (*Con*) or transiently transfected with a plasmid encoding α-synuclein (*Syn*) or parkin (*PRK*), separately. After 48 h of incubation, total cell lysates were obtained in 1× lysis buffer containing Triton X-100, and the expression of each protein was confirmed by Western blot analysis with either anti-Myc or anti-α-synuclein antibodies (*α-Syn*), as indicated. B. Where specified, H19-7 cells were mock-transfected or transiently transfected with either a plasmid encoding 1 μg of α-synuclein (*pSyn*) alone or with the same plasmid plus a cDNA construct (1 or 5 μg) to express wild type parkin (*pPRK*) for 48 h, as indicated. After the cell lysates were isolated, Western blot analysis was performed with monoclonal anti-α-synuclein antibodies. *C*, H19-7 cells were transiently transfected with the plasmids encoding α-synuclein (*pSyn*, *α-S*) and/or parkin (*pPRK*), as indicated. After 24 h, the cells were washed in PBS, incubated with methionine-free DMEM plus [^{35}S]methionine (10 μCi/ml) for 8 h and washed in PBS. Next the cells were washed extensively with DMEM, incubated for the indicated times, and lysed in TLB. Primary antibody against α-synuclein was added to the cell lysates, and protein A-Sepharose bead mixtures were added and incubated for an additional 1 h. Immunoprecipitated samples were washed three times in lysis buffer and solubilized by boiling samples for 5 min. After electrophoresis, the gel was stained with Coomassie Blue dye, dried, and analyzed by autoradiography. *D*, H19-7 cells were untreated (*C*) or transiently transfected with plasmids to express wild type α-synuclein (*S*, *α-S*, or *α-Syn*) and/or parkin (*P*), as indicated. The cell lysates were incubated with monoclonal anti-α-synuclein antibody or anti-p53 IgG at 4 °C overnight, and protein A-Sepharose beads were added to the cell lysates for 2 h at 4 °C with gentle rotation. Bound proteins were dissociated by boiling, and the protein samples were separated through a 15% SDS-PAGE gel and immunoblotted with either monoclonal antibody against α-synuclein or monoclonal anti-*O*-GlcNAc antibody, as indicated. *E*, parkin-mediated disintegration of intracellular granular accumulation caused by transient transfection of α-synuclein. Where indicated, H19-7 cells were transiently transfected with the plasmid encoding α-synuclein or/and parkin for 2 days and immunostained with an antibody specific to α-synuclein.

polyubiquitinated green fluorescent protein (GFP)-based reporter system as a proteasomal target protein (26). In this system, ubiquitin fusion degradation signals, with a mutated noncleaving ubiquitin moiety, were attached to a stable jellyfish GFP and therefore converted into a substrate for ubiquitin-proteasome-dependent proteolysis. Plasmid, pUb^{G76V}GFP, was constructed and used for this purpose, in order to measure the activity of the ubiquitin-proteasome pathway in living cells. The activity of proteasome can be measured by means of the emitted fluorescence from GFP. If the ubiquitin-GFP fusion proteins are rapidly degraded through the proteasome pathway, green fluorescence should not be detected. However, if they are not degraded, accumulated levels of green fluorescence should be detected. First, the plasmid encoding Ub^{G76V}GFP was transiently transfected into H19-7 cells, and then the cells were treated with the proteasome inhibitor, clastolactacystin β-lactone. As expected, the fluorescence levels of the GFP-reporter construct increased as a result of the activity of the native proteasomal degradation machinery being blocked in the H19-7 cells (Fig. 6*A*, *a* and *c*), confirming that 10 μM clastolactacystin β-lactone is sufficient to efficiently block the intracellular proteasomal activity in H19-7 cells. When the cells were co-transfected with Ub^{G76V}GFP plus parkin, the mean fluorescence intensity of the cells significantly decreased (Fig. 6*A*, *a* and *b*). As described above, it is presumed that parkin activates the ubiquitination process of ubiquitin-GFP fusion proteins as an E3 protein ligase or that it affects the proteolytic enzyme activity of either proteasome or other protease(s). The possibility that parkin induces the activation of the proteolytic proteasomal machinery was tested in the presence of proteasome inhibitor. Compared with control cells transfected with parkin alone, the addition of clastolactacystin β-lactone did not block the parkin-induced degradation of ubiquitin-GFP, and a significantly reduced level of Ub^{G76V}GFP

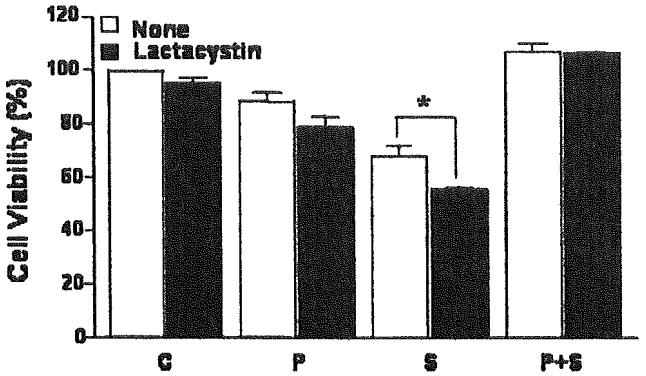

FIG. 5. **The neuroprotective effect of parkin against α-synuclein is exerted via proteasome-independent pathway(s).** Where specified, H19-7 cells were mock-transfected (*C*) or transiently transfected with a plasmid encoding parkin (2.5 μg) or α-synuclein (2.5 μg), respectively, or co-transfected with plasmids to express parkin and α-synuclein, together (*S* + *P*). The cells were then untreated (*None, open bar*) or stimulated with 10 μM proteasome inhibitor, clastolactacystin β-lactone, for 12 h (*Lactacystin, closed bar*), and cell viability was estimated with MTT extraction assay. *, $p < 0.05$

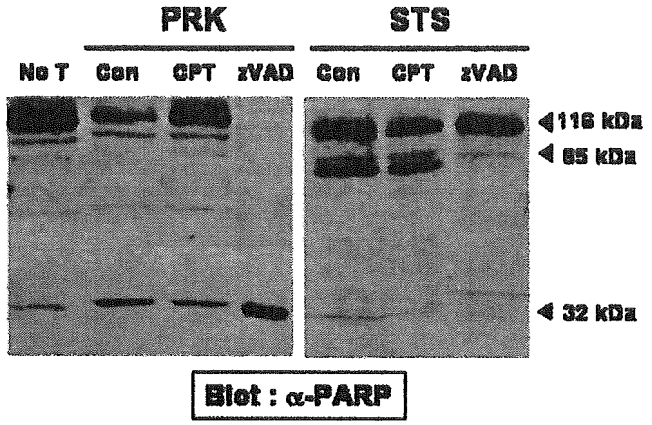

FIG. 7. **Parkin activates novel PARP-cleaving protease in hippocampal progenitor cells.** After H19-7 cells were mock-transfected or transiently transfected with 5 μg of plasmid encoding wild type parkin, the cells were untreated or stimulated with either calpeptin (50 μM, *CPT*) or *Z*-VAD-fmk (30 μM) for 12 h, as indicated. Where specified, mock-transfected cells were stimulated with 1 μM staurosporine (*STS*) for 12 h. Total cell lysates were resolved by SDS-PAGE and analyzed by Western blotting analysis with anti-PARP antibodies. The intact PARP and its proteolytic fragments are denoted by the *arrows*.

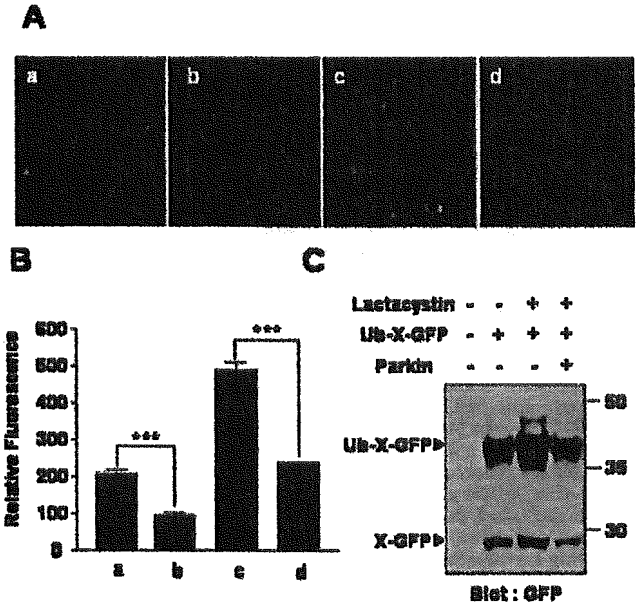

FIG. 6. **Parkin promotes the degradation of polyubiquitinated GFP fusion protein (Ub^{G76V}GFP) via a proteasome-independent pathway.** *A*, where indicated, H19-7 cells were transiently transfected with either 5 μg of plasmid encoding ubiquitinated green florescent protein (Ub^{G76V}-GFP) alone (*a* and *c*) or the same plasmid plus 5 μg of a cDNA construct to express wild type parkin (*b* and *d*). Then the cells were either untreated (*a* and *b*) or stimulated with 10 μM proteasome inhibitor, clastolactacystin β-lactone for 12 h (*c* and *d*), and the relative fluorescence levels from the GFP proteins were observed by using a low magnification fluorescence micrograph. *B*, after each cell lysate was prepared by using 1× lysis buffer containing 1.0% Triton X-100, the relative fluorescence levels from each sample were quantified by measuring at $\lambda_{EX} = 480/\lambda_{EM} = 510$. ***, $p < 0.001$. *C*, Western blot analysis was performed by using anti-GFP antibodies. Polypeptides with sizes corresponding to the cleaved products and the uncleaved precursors are indicated as X-GFP and Ub-X-GFP, respectively.

fluorescence was observed (Fig. 6*A*, *c* and *d*). This result shows that parkin appears to stimulate a novel proteasome-independent degradation process of the ubiquitinated-GFP fusion protein.

To assess the presence of ubiquitinated-GFP fusion protein, Western blot analysis was performed using anti-GFP antibodies. As shown in Fig. 6*C*, most of the Ub-X-GFP proteins were greatly ubiquitinated, and only small amounts of cleaved GFP protein were expressed as a result of the deubiquitination process. Consistent with Fig. 6*B*, the protein levels of ubiquitinated GFP also increased in the presence of lactacystin, and the overexpression of parkin led to a significant decrease of up-regulated levels of GFP proteins in the presence of lactacystin. Moreover, the nonubiquitinated GFPs as well as ubiquitinated GFPs were equally digested by parkin overexpression, suggesting that the ubiquitination process appears not to be a prerequisite for its degradation by the nonproteasomal pathway.

Transient Transfection of Parkin Causes the Activation of Cysteine Protease, Calpain, in H19-7 Cells—Next, we attempted to investigate whether any intracellular protease(s), other than the proteasome system, could be activated by parkin. First, to test whether the overexpression of parkin induces caspase(s), the occurrence of possible cleavage in PARP was determined after its transient transfection into H19-7 cells (Fig. 7). Generally, active caspase-3, -6, -7, -8, and -10 induce the cleavage of PARP in response to various proapoptotic inducers. As a positive control, the addition of the Ser/Thr kinase inhibitor, staurosporine, resulted in the cleavage of PARP via the activation of caspase and generated a typical 85-kDa fragment of PARP in H19-7 cells. However, the overexpression of parkin generated a novel cleavage pattern of PARP, in which PARP was cleaved into a 32-kDa fragment but not into the typical 85-kDa fragment (Fig. 7). Based on the previous report that the non-caspase-mediated atypical cleavage of PARP occurs via the cysteine protease, calpain, during the formation of selenite cataract (27), the possible activation of calpain and its effect on cell viability was investigated in response to parkin. Plasmid encoding wild type parkin was transfected into H19-7 cells, and the cells were incubated for 2 h with 50 μM calpeptin, a chemical inhibitor of calpain. The analysis of the cell lysates was done by Western blot analysis with anti-PARP antibody. When intracellular calpain activity was suppressed by calpeptin, the cleavage of intact 116-kDa PARP into its 32-kDa fragment was significantly suppressed (Fig. 7). This finding suggested that the parkin-induced novel fragmentation of PARP occurred via the activation of calpain but not that of caspase. In support of this conclusion, when cells were pretreated with a typical, cell-permeable inhibitor of caspase, *Z*-VAD6, the generation of the parkin-mediated novel PARP fragment was

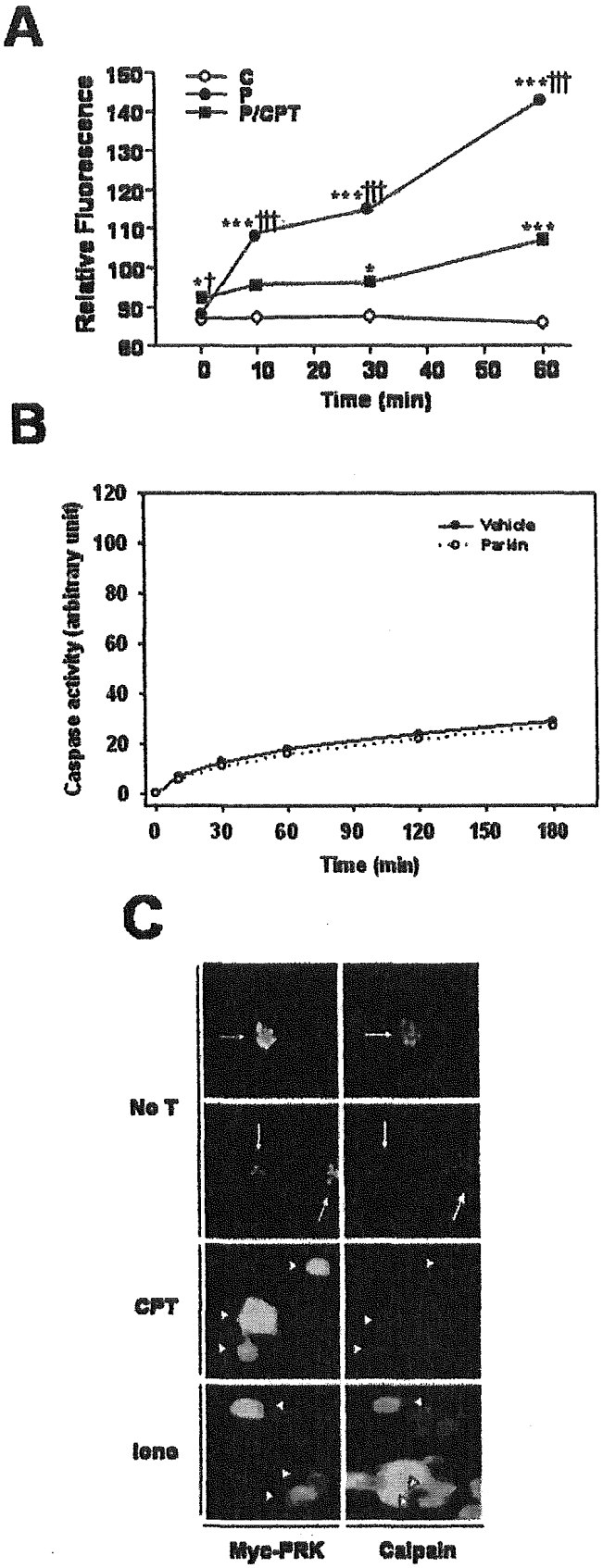

FIG. 8. **Transient transfection of parkin increases intracellular calpain activity, but not caspase, in H19-7 cells.** Where indicated, H19-7 cells were mock-transfected (*Vehicle*) or transiently transfected with 5 μg of pcDNA3.1-Parkin-Myc vector (*P*). Prior to assay of calpain activity, 50 μM calpain inhibitor, calpeptin, was added to the cells transfected with a plasmid encoding parkin (*P/CPT*). The prepared cell lysates were incubated with either Suc-LLVY-AMC peptide (80 μM) as a calpain substrate (*A*) or Ac-DEVD-*p*NA (10 μM) as a substrate for caspases (*B*). The amount of cleaved AMC fragments was measured at $\lambda_{EX} = 380/\lambda_{EM} = 460$ (*, $p < 0.05$; ***, $p < 0.001$ *versus* C; †, $p < 0.05$; †††, $p < 0.001$ *versus* P/CPT), and the cleavage of *p*NA via active caspase was measured colorimetrically at 405 nm. In *C*, the H19-7 cells were plated onto microscope coverslips placed in 6-well culture plates, were transfected with 5 μg of Myc-Parkin plasmid for 24 h, and were washed twice with RPMI 1640 medium, and fresh culture medium was added without or with calpeptin (*CPT*) or ionomycin (*Iono*). Immunofluorescence microscopy was used to determine Myc-parkin-expressing cells by using anti-Myc primary and rhodamine-labeled secondary antibody in the *left panel*. In the *right panel*, endogenous calpain activity was measured by using membrane-permeable and fluorogenic calpain substrate, Boc-Leu-Met-7-amino-4-chloromethylcoumarin, as described under "Experimental Procedures." In all figures, experiments were performed at least twice with similar results.

greatly enhanced in H19-7 cells, whereas staurosporine-induced PARP cleavage was completely blocked by Z-VAD-fmk but not by calpeptin (Fig. 7).

To confirm whether the overexpression of parkin augments calpain or caspase activity, intracellular calpain and caspase activities were measured after the transient transfection of parkin in H19-7 cells. Suc-LLVY-AMC (28) was used as a substrate for calpain, whereas a colorimetric substrate, Ac-DEVD-*p*NA, was used for active caspase. After the cells were transfected with a plasmid encoding parkin, the cells were washed with PBS buffer two times, and the medium was replaced with DMEM without phenol red. Prior to the calpain assay, 80 μM Suc-LLVY-AMC was added to each well, and the fluorescence intensity of the cleaved AMC fragments was measured after different lengths of time. For the assessment of the caspase activity, 10 μM Ac-DEVD-*p*NA was added, and the cleavage of *p*NA was monitored colorimetrically at 405 nm. When parkin was overexpressed in H19-7 cells, the fluorescence of AMC increased within 60 min, in comparison with the fluorescence of mock-transfected cells (Fig. 8*A*). In addition, the parkin-induced hydrolysis of Suc-LLVY-AMC was significantly suppressed in the presence of the calpain inhibitor, calpeptin (Fig. 8*A*), indicating that parkin increases the degradation of the fluorogenic substrate, Suc-LLVY-AMC, by the activation of intracellular calpain. Meanwhile, the overexpression of parkin did not stimulate caspase activity in a significant way, compared with the mock-transfected control cells (Fig. 8*B*).

Subsequent to examining the effects of parkin on calpain activity *in vitro*, measurements were done on single neuronal cells where the individual cells were overexpressing parkin to correlate these findings with events that occur *in situ* or *in vivo*. Lipid-soluble Boc-Leu-Met, conjugated to the GSH-binding fluorophore, 7-amino-4-chloromethylcoumarin, was utilized to provide a membrane-permeant calpain substrate. On entering the cell, this compound is conjugated to GSH by glutathione transferase, therefore trapped in the cell. This allows measurement of intracellular calpain activity, since GSH becomes linked to coumarin moiety, without affecting its fluorescence (29). The cells were transiently transfected with a vector to express Myc-parkin, subsequently followed by the assessment of its effect on calpain activity. Analysis of Myc-parkin-expressing fluorescent cells, which were distinguished by anti-Myc primary and rhodamine-labeled mouse secondary antibodies, showed that the overexpression of parkin causes a remarkable increase in calpain activity (Fig. 8*C*). Meanwhile, the cells treated with calpain inhibitors prior to measurement showed basal activity, compared with nontransfected control cells, whereas the exposure of ionomycin, as a positive control, resulted in a remarkable induction of endogenous calpain activ-

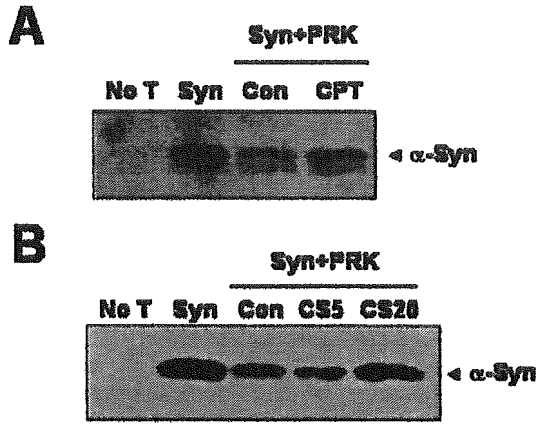

FIG. 9. **Parkin-induced degradation of α-synuclein is blocked by calpain inhibitor.** Where indicated, H19-7 cells were mock-transfected (*C*) or transiently transfected with 5 μg of plasmid encoding either α-synuclein (*pSyn*) alone or α-synuclein plus parkin construct (*Syn + PRK*), respectively. The cells were then either untreated (*No T*) or stimulated with calpain inhibitor, 50 μM calpeptin (*CPT*) (*A*) or the indicated concentration of calpastatin peptide (CS5, 5 μM; CS20, 20 μM) (*B*) for 4 h. Total cell lysates were resolved by SDS-PAGE and analyzed by Western blotting analysis using the antibodies against α-synuclein.

ity, irrespective of the expression the parkin, indicating that the assay method we used corresponded well with intracellular calpain activity (Fig. 8*C*). Overall, our data suggest that parkin activates the proteasome-independent cysteine protease, calpain, but not caspase, in neuronal H19-7 cells.

Parkin Induces the Degradation of α-Synuclein via the Activation of Calpain in H19-7 Cells—In previous studies, we and Eberz *et al.* (30, 31) reported that calpain degrades α-synuclein *in vitro*. Next, we evaluated whether parkin-induced calpain activation is involved in the degradation of α-synuclein *in vivo*. The H19-7 cells were transfected with a plasmid encoding parkin or/and α-synuclein, respectively. Intracellular levels of α-synuclein and its degradation were measured by Western blot analysis using anti-α-synuclein IgG. As shown in Fig. 9, compared with co-transfection with α-synuclein alone, co-transfection of the cells with α-synuclein plus parkin potentiated the degradation of α-synuclein in proportion to the amount of parkin DNA transfected. In addition, the scavenging effect of parkin on the degradation of α-synuclein was significantly blocked in the presence of calpain inhibitors, such as either calpeptin (Fig. 9*A*) or calpastatin peptide, a 27-residue cell-permeable peptide encoded by exon 1B of human calpastatin (Fig. 9*B*). These findings indicated that parkin potentiates α-synuclein degradation via the activation of calpain in H19-7 cells. To clarify whether the cytoprotective effect of parkin on α-synuclein-induced cell death is derived from removal of α-synuclein, through calpain activation, the cell viability of H19-7 cells was determined during the blockade of calpain activity. When H19-7 cells were transiently transfected with either construct encoding α-synuclein alone or α-synuclein plus parkin, the protective effect of parkin on α-synuclein-induced cytotoxicity was significantly decreased in the presence of calpeptin (Fig. 10*A*) or calpastatin peptide (Fig. 10*B*). As a control, the addition of each calpain inhibitor alone did not produce any significant effect on cell viability (Fig. 10). These results clearly show that parkin potentiates the degradation of α-synuclein, via the activation of calpain, which sequentially rescues the neuronal hippocampal cells from a α-synuclein-induced neuronal cell death.

DISCUSSION

The presynaptic protein, α-synuclein, is a major component of heavily-ubiquitinated cytoplasmic inclusions, LBs, that are

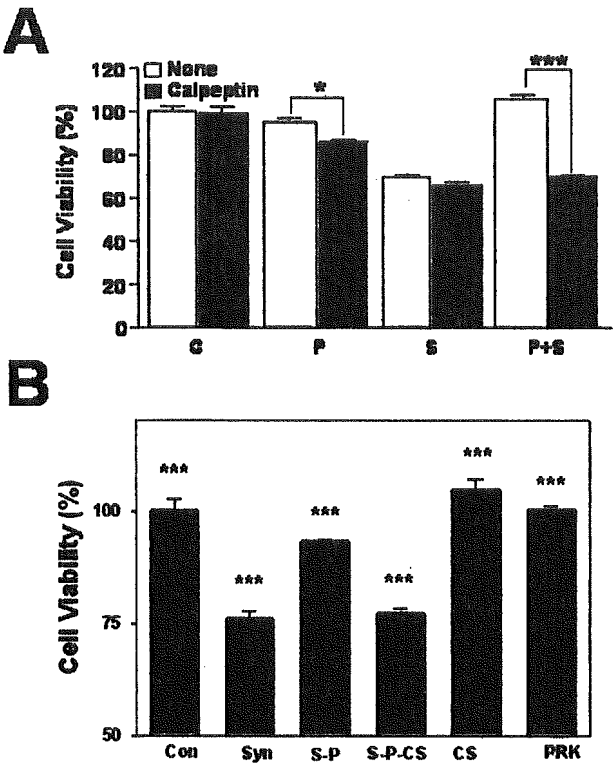

FIG. 10. **The neuroprotective effect of parkin against α-synuclein involves calpain in H19-7 cells.** Where indicated, H19-7 cells were mock-transfected (*C* or *Con*) or transiently transfected with 2.5 μg of pcDNA-parkin-Myc construct cDNA (*P* or *PRK*) or pcDNA3-α-synuclein (*S* or *Syn*), respectively, or co-transfected with parkin expression vector plus a plasmid encoding α-synuclein (*P + S* or *S-P*). The cells were treated with 50 μM of calpeptin (*A*) or calpastatin inhibitor (*CS* in *B*) for 12 h to block intracellular calpain activity (*black bar*). Cell viability was determined by the MTT extraction method. *, $p < 0.05$; ***, $p < 0.001$.

the pathological hallmarks of sporadic PD and of one particular subgroup of familial PD (5, 32). Although little is known about the neurobiology of α-synuclein, two mutations in this gene (A53T and A30P) cause autosomal dominant familial PD (4, 33). In the present study, we attempted to elucidate the regulatory role of parkin in α-synuclein-induced neuronal cell death in hippocampal H19-7 cells. Our findings indicate that α-synuclein selectively binds to parkin in hippocampal neuronal cells. The binding between α-synuclein and parkin is dependent on the N-terminal ubiquitin-like domain of parkin. In addition, the overexpression of parkin saved the H19-7 cells from α-synuclein-induced cytotoxicity.

Parkin is responsible for the autosomal recessive form of early onset PD (AR-JP), and the impairment of proteasome activity is observed in those patients suffering from AR-JP (34). The ubiquitin-proteasome pathway is implicated in the degradation of intracellular proteins that control so many vital processes, such as cell cycle progression, signal transduction, differentiation, and apoptosis. Ub is covalently attached to target proteins for degradation. The protein-ubiquitination process is catalyzed by three enzymes, E1, E2, and E3, to form a poly-Ub chain that serves as the degradation signal for proteolytic attack by the 26 S proteasome (35, 36). To date, parkin is known to interact with the ubiquitin-conjugating enzyme E2 and is functionally linked to the ubiquitin-proteasome pathway as an ubiquitin ligase E3.

Based on the functional role of parkin, we thought that the cytoprotective effect of parkin on α-synuclein-induced cell death could be derived from its ubiquitin ligase activity,